

---

**N7811368**

---

---

# **STRAPDOWN GYRO TEST PROGRAM**

**TELEDYNE SYSTEMS CO., NORTHRIDGE, CALIF**

**OCT 1977**



# **STRAPDOWN GYRO TEST PROGRAM FINAL REPORT**

**(1 JUNE, 1976 to 1 SEPTEMBER, 1977)**

**OCTOBER 1977**

**BY**

**R.B. IRVINE  
R. VAN ALSTINE**

**PREPARED UNDER CONTRACT NAS8-31909  
FOR THE  
GEORGE C. MARSHALL SPACE FLIGHT CENTER, ALABAMA, 35812  
BY**

** TELEDYNE SYSTEMS COMPANY**  
19601 Nordhoff St. • Northridge, Calif. 91324



UNCLASSIFIED

SECURITY CLASSIFICATION OF THIS PAGE (When Data Entered)

REPORT DOCUMENTATION PAGE		READ INSTRUCTIONS BEFORE COMPLETING FORM
1. REPORT NUMBER ADTC TR 77-3 (Vol 1)	2. GOVT ACCESSION NO	3. RECIPIENT'S CATALOG NUMBER
4. TITLE (and Subtitle) Eighth Guidance Test Symposium Proceedings		5. TYPE OF REPORT & PERIOD COVERED Symposium Proceedings
		6. PERFORMING ORG. REPORT NUMBER TR 77-3 (Vol 1)
7. AUTHOR(s) As indicated on individual papers.		8. CONTRACT OR GRANT NUMBER(s)
9. PERFORMING ORGANIZATION NAME AND ADDRESS 6585th Test Group/GD Holloman AFB, New Mexico 88330		10. PROGRAM ELEMENT PROJECT, TASK AREA & WORK UNIT NUMBERS
11. CONTROLLING OFFICE NAME AND ADDRESS 6585th Test Group/GD Holloman AFB, New Mexico 88330		12. REPORT DATE May 1977
		13. NUMBER OF PAGES 732
14. MONITORING AGENCY NAME & ADDRESS (if different from Controlling Office)		15. SECURITY CLASS. (of this report) Unclassified
		15a. DECLASSIFICATION/DOWNGRADING SCHEDULE
16. DISTRIBUTION STATEMENT (of this Report)		
17. DISTRIBUTION STATEMENT (of the abstract entered in Block 20, if different from Report)		
18. SUPPLEMENTARY NOTES		
19. KEY WORDS (Continue on reverse side if necessary and identify by block number) Gyroscopes, accelerometers, modeling, guidance, inertial, navigators		
20. ABSTRACT (Continue on reverse side if necessary and identify by block number) These proceedings contain papers included in the Eighth Biennial Guidance Test Symposium. This symposium, hosted by the Central Inertial Guidance Test Facility, is directed toward the exchange of information, stimulation of new ideas, and discussion of recent developments in the field of guidance testing. The papers presented in these proceedings include such topics as aircraft inertial navigators, strapped-down guidance systems, component evaluation, and analysis techniques. The included papers were those presented in the		

**UNCLASSIFIED**

**SECURITY CLASSIFICATION OF THIS PAGE(When Data Entered)**

unclassified sessions of the symposium. Papers presented in the classified portion of the meeting are being published as Volume II.

**UNCLASSIFIED**

**SECURITY CLASSIFICATION OF THIS PAGE(When Data Entered)**

## TABLE OF CONTENTS

<u>Paragraph</u>		<u>Page</u>
I	SCOPE .....	1
II	INTRODUCTION.....	1
III	HARDWARE DESCRIPTION.....	1
IV	TESTING .....	1
V	CONCLUSIONS .....	2
VI	RECOMMENDATIONS .....	2
APPENDIX A .....		A-1
APPENDIX B .....		B-1
APPENDIX C .....		C-1





## I. SCOPE

This report summarizes the work accomplished and testing performed using the equipment provided by the NASA Marshall Space Flight Center under the no-cost Contract, Number NAS 8-31909, during the period of 1 June, 1976 through 1 September, 1977.

## II. INTRODUCTION

The primary purpose of the testing conducted which utilized the GFE provided under this contract was to determine the power spectral noise characteristic performance of the Teledyne two-degree-of-freedom dry tuned-gimbal gyroscope. These tests were conducted using a current configuration SDG-5 Gyro in conjunction with the NASA Marshall SPC provided test equipment with minor modification. Additionally, some long term bias stability tests were conducted on Gyro S/N 606 as well as some first-difference performance testing at the Martin Marietta Corporation - Denver facility.

## III. HARDWARE DESCRIPTION

The descriptions of the gyro, test equipment and the testing performed utilizing this hardware are contained in Appendix A. The SDG Test Electronics Box caging electronics was modified for the 7 Hz bandwidth requirements of DRIRU II. The block diagrams and Bode plot characteristics of the capture loops are described in Appendix A, Section III, Figures 4, 5, 6 and 7.

## IV. TESTING

The PSD testing performed is described in Appendix A, Section 4. In addition, first difference performance tests were conducted on Gyro Serial Number 069 at the Martin Marietta Corporation - Denver facility. This data is presented in Appendix B along with appropriate definitions. Finally, some long term bias stability data taken at Teledyne at an earlier date on Gyro S/N 606 is presented in Appendix C.

## V. CONCLUSIONS

The general conclusions from the PSD testing performed are presented in Appendix A, Section VIII. It was concluded from this test series that the SDG-5 Gyro as a sensor would meet the equivalent noise angle performance requirements for DRIRU II. These tests were a significant milestone that led to Teledyne's selection as the contractor for the DRIRU II development.

It may be concluded from the first-difference test data of Appendix B, that the Teledyne SDG-5 Gyro is an excellent sensor for gyro-compass of self-contained alignment inertial systems.

The long term bias data presented in Appendix C shows excellent stability over a three year period which will result in minimal recalibration requirements for the sensor when implemented in DRIRU II.

## VI. RECOMMENDATIONS

It is recommended that the GFE hardware used in this contract be dispositioned to the DRIRU II Contract for use and support of further testing for new requirements as they arise.

APPENDIX A



**EIGHTH BIENNIAL GUIDANCE TEST SYMPOSIUM**

**AN EXAMINATION OF LOW POWER SPECTRAL DENSITY (PSD)  
NOISE PERFORMANCE OF A DRY TUNED GIMBAL  
TWO-DEGREE-OF-FREEDOM GYROSCOPE, AND  
METHODS FOR FURTHER NOISE REDUCTION**

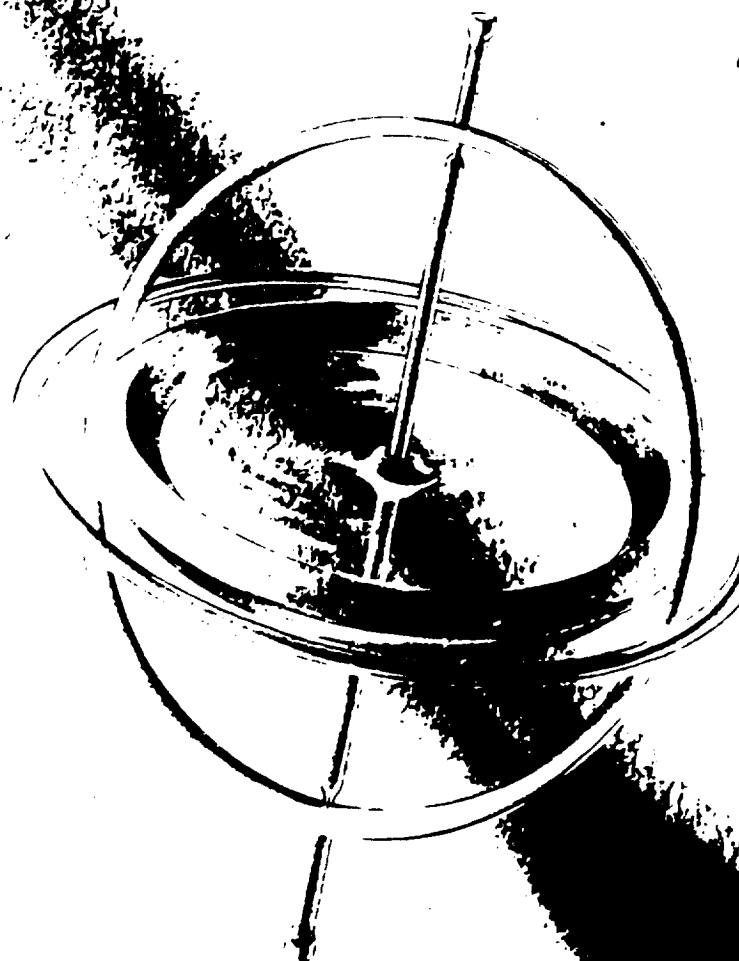
**AUTHORS: ROBERT B. IRVINE  
JOHN W. RITTER**

 **TELEDYNE SYSTEMS COMPANY**  
19601 Nordhoff St. • Northridge, Calif. 91324



VOLUME 1

ADTC TR 77-3



**EIGHTH  
GUIDANCE TEST  
SYMPOSIUM  
PROCEEDING**



APPROVED FOR PUBLIC RELEASE  
DISTRIBUTION UNLIMITED.





## ABSTRACT

Recent test and evaluation of dry, tuned gimbal, two-degree-of-freedom gyroscopes has revealed power spectral "noise" levels that compare favorably with floated gyro standards currently used in high accuracy pointing and attitude stabilization systems. Power spectral density test data on the Teledyne SDG-5 dry tuned gyroscope are presented and compared with published results for single-degree-of-freedom floated gyroscopes. The specific capabilities and limitations of the dry tuned gyro approach for high accuracy pointing applications are discussed.

Gyro noise in the strictest sense may be defined as that component of the angular rate output which does not represent the measurement of the true angular rate input to the gyroscopic sensor, but is a spurious output resulting from sensor imperfections, including the associated control and output interface electrical circuitry. The principal sources of the noise for either floated or dry-tuned gyros may be categorized as follows:

1. Suspension system induced torques.
2. Non-suspension system induced torques.
3. Electrical/Magnetic field noise.

The predominant source of low frequency angular rate noise present in inertial gyros results from angular motions or misalignments of the driven (spin reference) axis with respect to the case fixed (stationary) axes. These motions (which ideally do not exist), although small, result in suspension system induced torques acting upon the rotor, or "noise".

It is shown that it is possible to effect significant reductions in this dominant source of noise by the optimization of the basic design parameters of the dry-tuned gyroscope. In particular, it is shown that this noise reduction is most sensitive to the ratios of rotor inertias to gimbal inertias, as well as to the number of gimbals utilized in the design. Tradeoffs of noise reduction versus gyro maximum shock/acceleration capability are presented. In addition further refinements related to angle pickoff accuracy considerations are described.

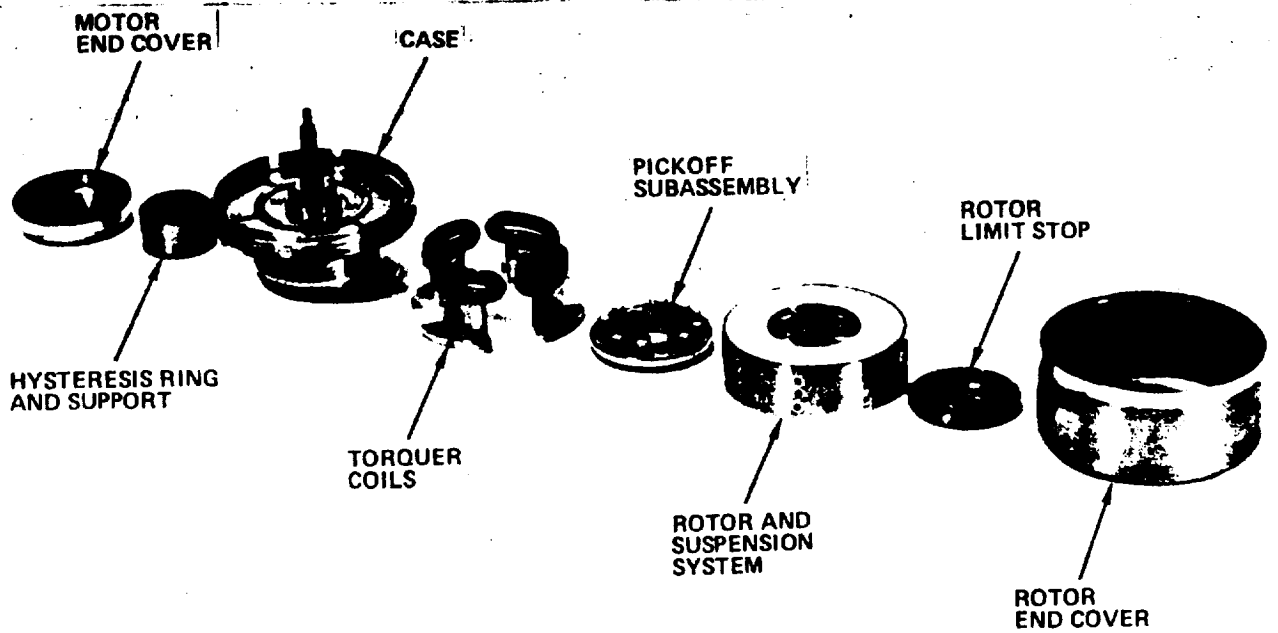
## I. INTRODUCTION

During calendar year 1976, Teledyne Systems Company initiated a program to accurately determine the spectral noise characteristic for the dry-tuned two-degrees-of-freedom SDG-5 Gyroscope. The demand for this data was quite sufficient from a number of potential users in such applications as high accuracy spacecraft stabilization (e.g. DRIRU II and Space Telescope), high energy laser (HEL) pointing, and a number of other important applications. Initial testing was conducted in-house early in the program where it was determined that more sophisticated data acquisition systems were desirable and, primarily that higher stability well instrumented test piers would be required. Teledyne then contacted the Martin-Marietta Corporation, Denver, Colorado and the Space and Missile Systems Organization (SAMSO), Los Angeles AFS, California where the SDG-5 was added to the list for test of candidates competing for the High Altitude Attitude Reference System (HAARS). Additional testing was accomplished at the Boeing Aerospace Company and at Lockheed Missiles and Space Company.

Sufficient data was obtained to show that the Teledyne SDG-5 gyroscope is an extremely attractive rate sensor for use in fine pointing control system applications where jitter is required in the milliarc-second region and that operate with bandwidths to 10 Hz. The instrument is particularly attractive in view of its high reliability, low relative cost to existing standards and capability of operation over a broad temperature range without the use of temperature control. No selection of instruments was made and units were tested on an "as available" basis. Standard laboratory analog rebalance loops were employed and no gyro heaters, precision temperature control or temperature compensation was used in the test series.

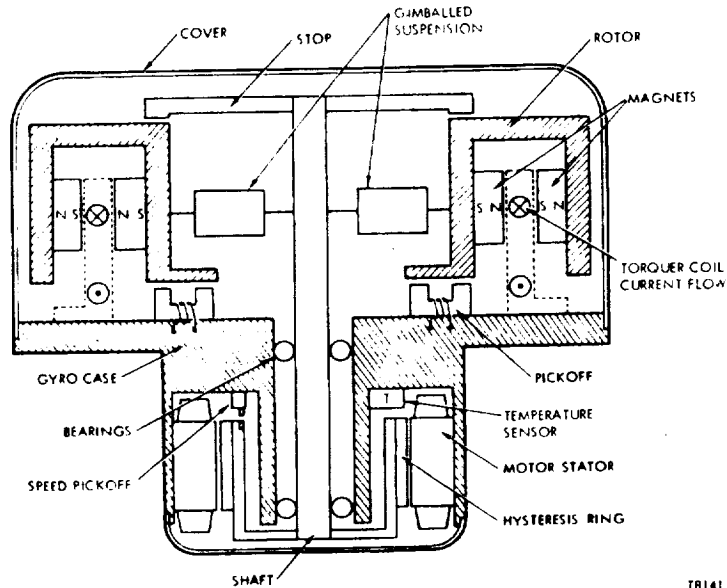
## II. GYRO DESCRIPTION

The Teledyne SDG-5 is a dry gyro and features an elastically supported rotor with a dynamically tuned suspension system. The two-degree-of-freedom strapdown gyro consists of four major subassemblies: the case, torquer coils, pickoffs, and rotor containing its tuned three-gimbal suspension system. These subassemblies are shown in Figure 1 and a schematic cross section of the gyro is shown in Figure 2. The gyro case supports a set of ball bearings which in turn carry the shaft. Mounted on one end of the shaft is the motor hysteresis ring and on the other end is the rotor and suspension system. The torquer coils and pickoff subassembly are attached to the case. The end covers, when soldered in place, provide the hermetic seal for the gyro.



PH1419A

Figure 1. SDG-5 Strapdown Gyro Subassemblies



TB1417

Figure 2. Schematic Cross-Section of the Strapdown Gyro

The Teledyne SDG-5 Gyro has an angular momentum of  $1 \times 10^6$  CGS units while operating at 6,000 RPM on standard R-4 size ball bearings. A summary of physical characteristics is presented in Table 1 and a summary of key performance characteristics is shown in Table 2.

Table 3 presents a summary of instrument characteristics [4] for single-degree-of-freedom floated gyros and a comparison of the SDG-5 two-degree-of-freedom dry gyro.

Table 1. Teledyne SDG-5 Gyro Characteristics

GENERAL

Weight	< 2.3 lbs
Size	3" dia x 3" long
Figure of Merit	320
g-Capability	150 g's
Rate Capability (Steady State)	100 °/sec

ROTOR

Mass of Rotor	260 GMS
Polar Moment of Rotor	1600 GM-CM <sup>2</sup>
Angular Momentum	1 x 10 <sup>6</sup> GM-CM <sup>2</sup> /sec

SUSPENSION

Tuned 3 gimbal

SPIN MOTOR

Type	Hysteresis Synchronous
Excitation Voltage (RMS sine wave, 3ϕ, 400 Hz)	30 volts
Run-Up Time	<30 seconds
Operating Power	2 watts

PICKOFF

Type	Variable Reluctance Transformer
Excitation Frequency	48K Hz sinewave
Excitation Voltage	7 VRMS
Nominal Scale Factor	100 V/RAD

TORQUER

Type	Voice Coil
Nominal Scale Factor	160 °/Hr/ma

HEATER - None Required

Table 2. Teledyne SDG-5 Gyro Performance Characteristics

Parameter	Units	Specification Value	Typical Value (mean)
<u>G-Insensitive Bias</u>			
Absolute Value	$^{\circ}/\text{Hr}$	$0 \pm 2.0$	$< 0.50$
Stability			
Continuous Operation (Random Drift)	$^{\circ}/\text{Hr } 1\sigma$	.001 Max.	0.0005
Shutdown Repeatability	$^{\circ}/\text{Hr } 1\sigma$	.01 Max.	0.0016
Temperature Cycle Stability	$^{\circ}/\text{Hr } 1\sigma$	-	0.0033
Temperature Sensitivity	$^{\circ}/\text{Hr}/^{\circ}\text{F}$	$0 \pm .002$	0.00059
<u>G-Sensitive Bias</u>			
Absolute Value	$^{\circ}/\text{Hr}/\text{G}$	$0 \pm 1.0$	$< 1.0$
Stability			
Continuous Operation (Random Drift)	$^{\circ}/\text{Hr}/\text{G } 1\sigma$	.002 Max.	0.0007
Shutdown and Temperature Cycle Repeatability	$^{\circ}/\text{Hr}/\text{G } 1\sigma$	-	0.008
Temperature Sensitivity	$^{\circ}/\text{Hr}/\text{G}/^{\circ}\text{F}$	$0 \pm .02$	0.0032
<u>Torquer Scale Factor</u>			
Absolute Value	$^{\circ}/\text{Hr}/\text{MA}$	150 Min.	160
Linearity	PPM Peak	100 Max.	25
Asymmetry	PPM Peak	-	3
Temperature Sensitivity	PPM/ $^{\circ}\text{F}$	$-230 \pm 20$	-229
<u>Axis Alignment</u>			
Absolute Value	$\widehat{\text{Sec}}$	60 Max.	30
Stability	$\widehat{\text{Sec}}$	-	10
<u>Angular Rate Capability</u>			
Steady State	$^{\circ}/\text{Sec}$	100	$>100$
Transient	$^{\circ}/\text{Sec}$	400	$>500$
Anisoelasticity	$^{\circ}/\text{Hr}/\text{g}^2$	$0 \pm .03$	.01
Gyro Time Constant	Seconds	100 Min.	200

T101556A

Table 3. Summary Comparison of Instrument Characteristics

Characteristics	Units	SII - Float-d Gyro [4]										TDF Dry Gyro	
		ICG VI No Wheel	ICG IV/5 Hemispherical Gas	ICG I/F-1/10 2 FRC/F-100	ICG I/F-100 Ball	25 IFC Spool Gas	14 IFC Spool Gas	GLI-111 Spool Gas	Norionics GLI-111 Spool Gas	GLI-111 Spool Gas	Honeywell GG 334 Spool Gas		Teledyne SDC-5 Ball
Wheel	Type												
II	km-cm/sec	0.5 x 10 <sup>6</sup>	0.7 x 10 <sup>6</sup>	1.7 x 10 <sup>6</sup>	1.7 x 10 <sup>6</sup>	0.54 x 10 <sup>6</sup>	0.15 x 10 <sup>6</sup>	1.4 x 10 <sup>6</sup>	1.4 x 10 <sup>6</sup>	0.2 x 10 <sup>6</sup>	0.2 x 10 <sup>6</sup>	1.0 x 10 <sup>6</sup>	
Speed	RPM	32,000	24,000	12,000	12,000	24,000	24,000	24,000	24,000	24,000	24,000	6,000	
Run Power	Watts	10.5	-12	1	1	5	5	5	5	5	5	2	
Gain I/C		NA	0.87	1.6	1.6	0	0.2	1	1	0.4	0.4	NA	
Characteristic Time (I/C) OA	Milli-sec	0.57	0.75	1	1	0.66	0.33	-1.0	4	0.5	0.5	NA	
Torque Generator	Type	EM (2 windings)	EM (2 windings)	EM (2 windings)	EM (2 windings)	EM	EM	EM	EM	EM	EM	PM	
Sensitivity	MERR	2.4/m <sup>2</sup>	2.4/m <sup>2</sup>	2.4/m <sup>2</sup>	2.4/m <sup>2</sup>	1/m <sup>2</sup>	1/m <sup>2</sup>	1/m <sup>2</sup>	1/m <sup>2</sup>	1/m <sup>2</sup>	1/m <sup>2</sup>	11 arc/ma	
Max Rate		100 crp	100 crp	40 crp	40 crp	100 crp	200 crp	110 crp	110 crp	110 crp	110 crp	100/sec	
Signal Generator	Type	EM E	EM E	EM E	EM E	EM	EM	EM	EM	EM	EM	EM	
Sensitivity	MV/MRAD/OA	NA	NA	NA	NA	2	20	20	40	24	24	100	
Suspension	Type	EM Tapered	EM Tapered	EM Tapered	EM Tapered	EM Tapered	EM Tapered	EM Tapered	EM Tapered	EM Tapered	EM Tapered	Tuned Global	
Radiat TC		8 min	8 min	8 min	8 min	8 min	8 min	8 min	8 min	8 min	8 min	NA	
Asial TC		3.4 hrs	3.4 hrs	3.4 hrs	3.4 hrs	3.4 hrs	3.4 hrs	3.4 hrs	3.4 hrs	3.4 hrs	3.4 hrs	NA	
Operating Temp	°F	121	135	135	135	135	132	140	170	180	180	0 to 200° F	
Mounting Configuration		End Stud	Fapered End Stud	End Stud	End Stud	Em Stud	Em Mounted	End Stud	Center Flange	Center Flange	Center Flange	Center Flange	
Environment:		NA	Misalt. Boost	Misalt. Boost	Satellite	Nitrate	Satellite	Cyco Compaasing	Navigator Satellite	30g max.	150g max.	150g max.	
Life Expectancy	MILIF (hrs)	NA	100K	100K	20K	100K	100K	100K	100K	NA	100K	100K	

\*Not Available  
\*\*Not Applicable

### III. SUPPORT ELECTRONICS

The SDG Electronics/Control Unit [6] contains the necessary analog rebalance electronics to cage both axes of the SDG-5. A photograph of the 19 inch rack-mounted panel is shown in Figure 3. Controls, located on the front panel are used to control the caging process and provide a convenient means for selecting various torque output scaling functions. Generally, the unit contains the necessary regulated and precision DC voltages, the gyro 48 kHz pickoff excitation, caging electronics and precision analog scaling electronics for each gyro axis. Refer to Figure 4 for the functional block diagram and to Figures 5 and 6 for measured cross and direct-axis control loop frequency response curves.

The previously described electronics was interfaced with the data acquisition system and the gyro mounted on the test pier as available at the various facilities. The functional organization utilized was as shown in Figure 7.

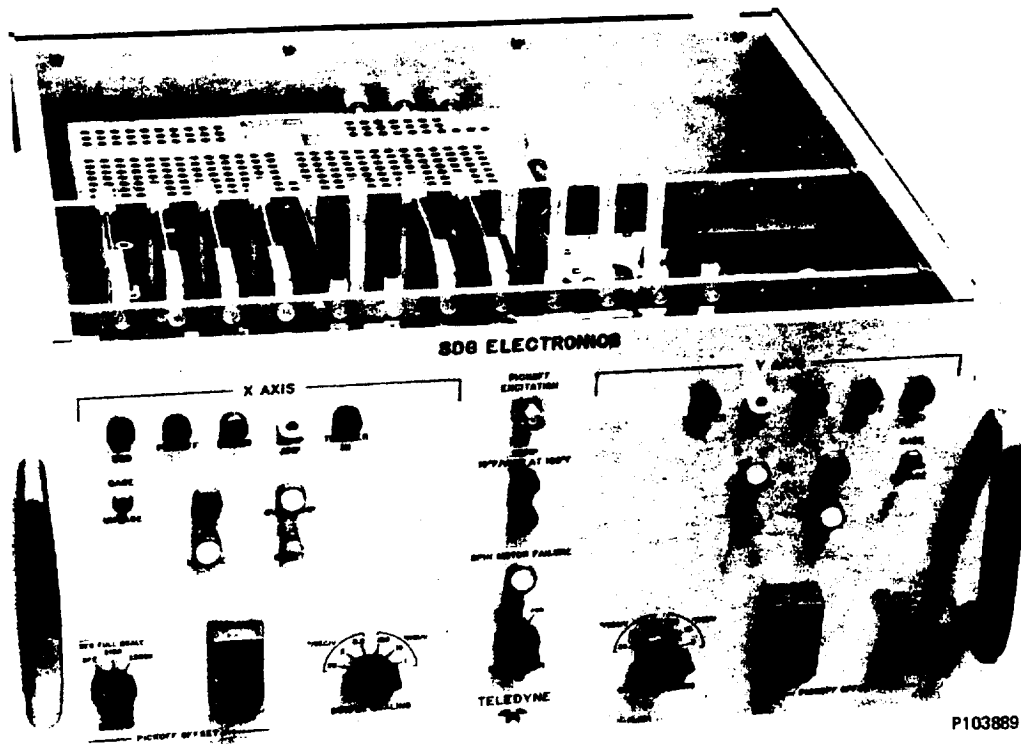
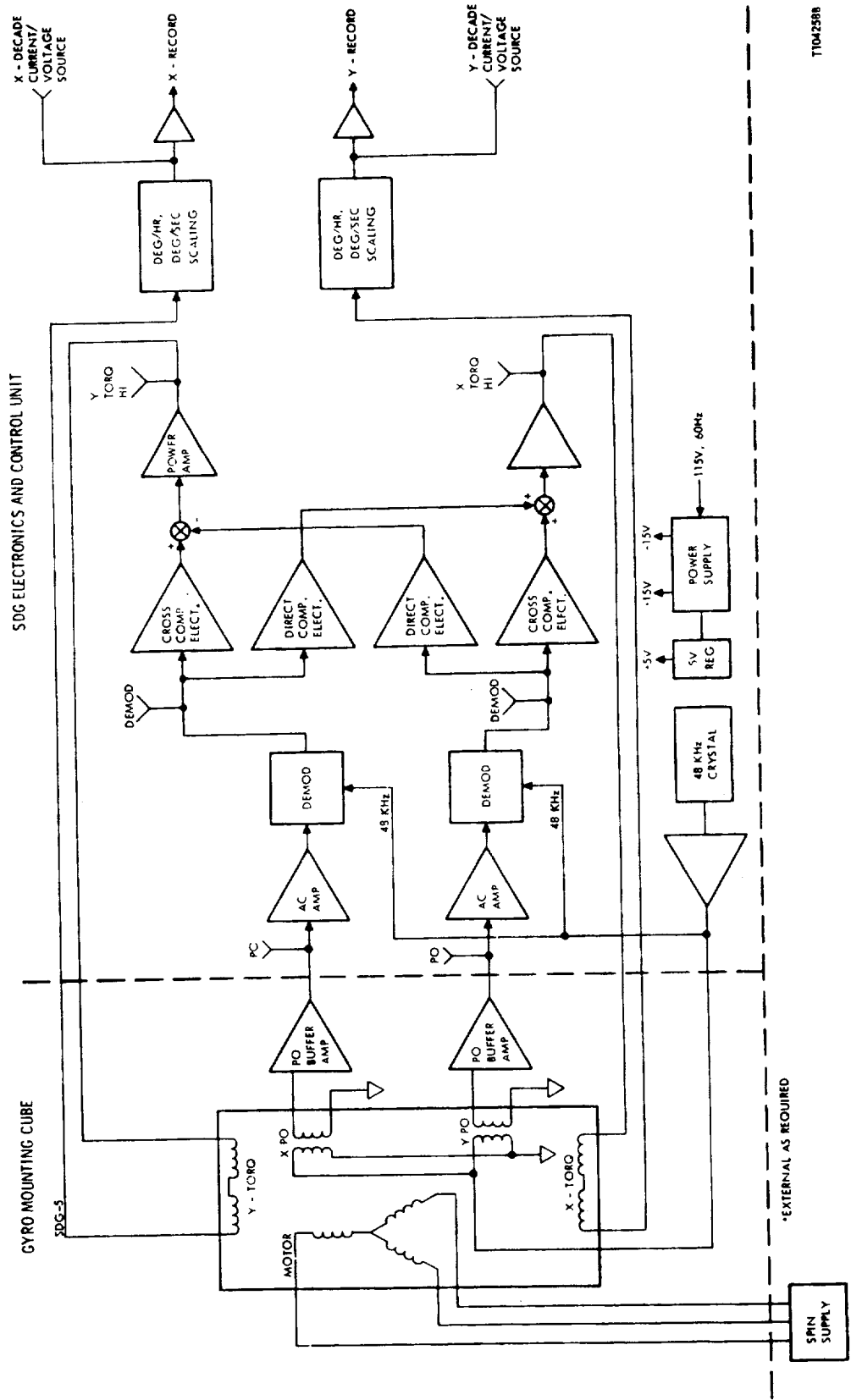


Figure 3. Teledyne Strapdown Gyro Laboratory Test Equipment [6]

ORIGINAL PAGE IS  
OF POOR QUALITY



T1042588

Figure 4. Functional Block Diagram of Teledyne Strapdown Gyro Test Mechanization



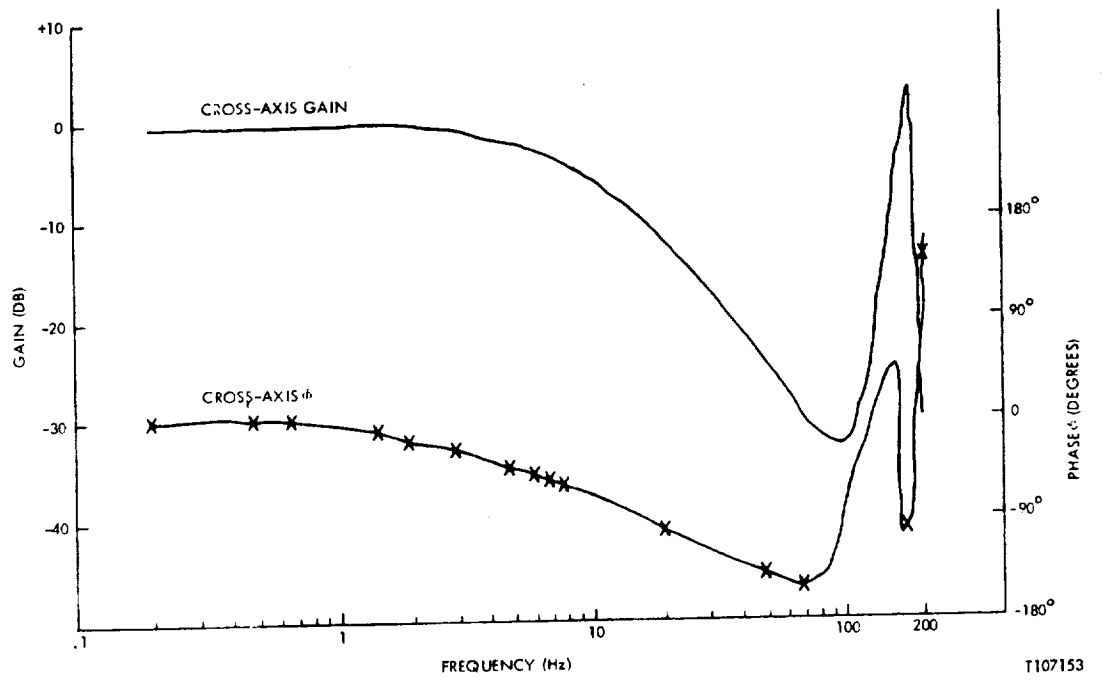


Figure 5. Cross Axis Bode Plot

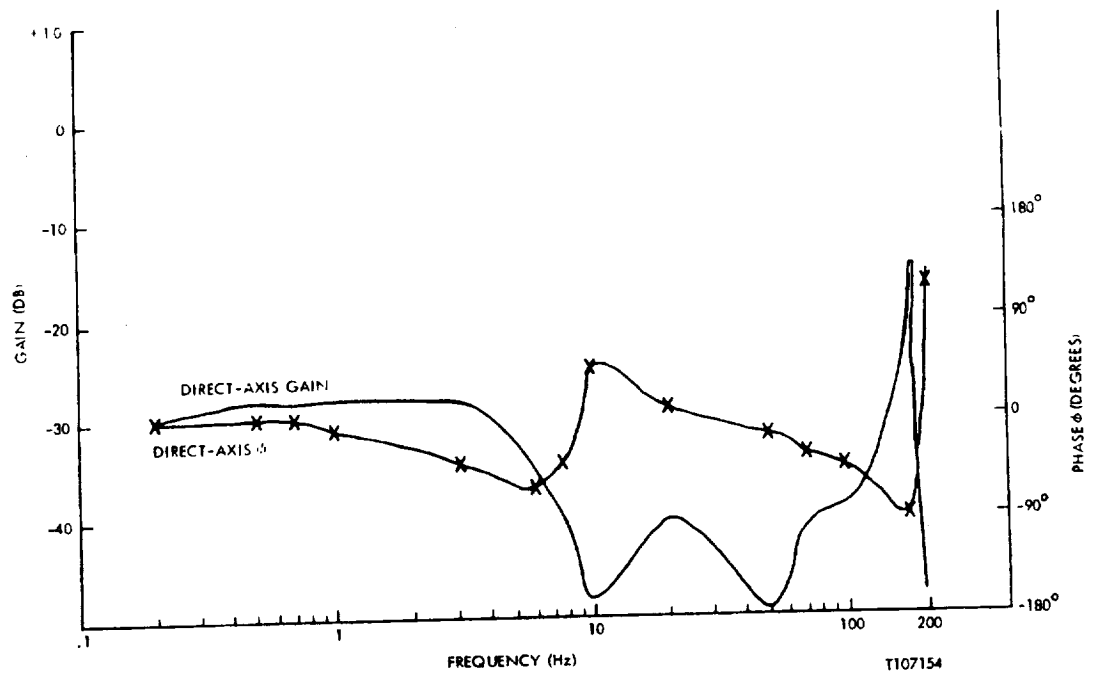
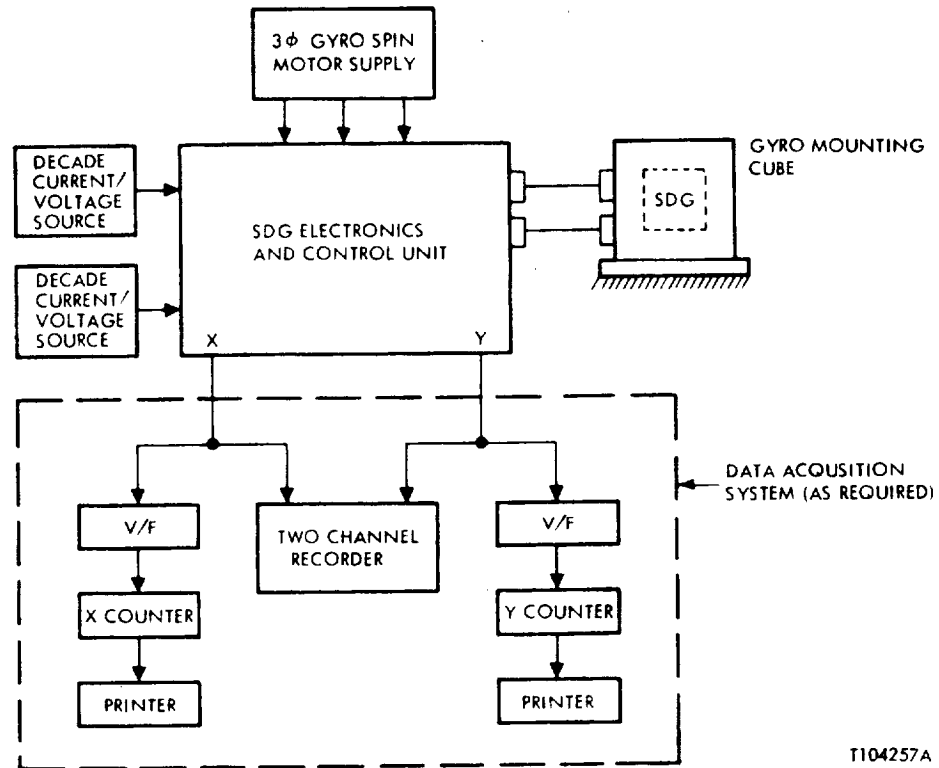


Figure 6. Direct Axis Bode Plot



T104257A

Figure 7. Teledyne Strapdown Gyro Test Setup with Data Acquisition System

#### IV. PSD TESTING PERFORMED

A total of 5 different SDG-5 gyros were used in the test program on an "as available" basis.

Table 4 presents a summary of the testing performed by facility. Most data was taken on SN 069 as it was evaluated by three facilities. Initial testing was performed at Boeing using analog rebalance loops of approximately 1 Hz bandwidth. This was subsequently increased to 7 Hz and standardized for the tests to follow in order to be representative of requirements on anticipated programs. In all cases, the data acquisition system and data reduction was provided by the test facility. Standard methods as described in the references [1], [2] were generally employed.

Table 4. Summary of PSD Testing Performed  
On Teledyne SDG-5 Gyro

Test Facility	No. Gyros Tested	Test Period	Gyro Test Equipment Used/ Coarse Loop Bandwidth	Data Acquisition System	Test Tier	Test Report
Boeing Aerospace Co. (Seattle, Wash.)	4 (SN's 014, 045, 068, 069)	21 July 1976 to 20 July 1976	Teledyne Strapdown Gyro Laboratory Test Equipment [1] (Standard Configuration) Analog Loop Approx 1 Hz	Omniferous FFT Analyzer Nicolet Scientific Corp Model 400A	Seismic Pad	Raw Data Available- No formal report anticipated
Martin-Marietta Corp. (Denver, Colorado)	2 (SN's 068, 069)	2 August 1976 to 26 October 1976	Teledyne Strapdown Gyro Laboratory Test Equipment [1] (Standard Configuration) Analog Loop Approx 7 Hz	MMC-A/D Converter [5]  PRIME Computer	MMC Granite Pier at south end of Fine Pointing Dimensionally Stable Simulator [5]	Spring 1977 [5] (Proprietary Report)
Holloman A. F. B. CIGTF (Alamogordo, N. M.)	1 (SN 069)	2 Sept. 1976 to 12 October 1976	As Above/7 Hz	Holloman-A/D Converter [1] III 2100 Computer	CIGTF Tilt Meter Instrumented Test Pad [1]	The Teledyne SDG-5 Gyro Test, Report No. TBD February 1977 [8]
Boeing Aerospace Co. (Seattle, Wash.)	1 (SN 069)	15 Oct 1976	As Above/7 Hz	Omniferous FFT analyzer Nicolet Scientific Corp. Model 400A	Seismic Pad and Lab Floor	Raw Data Available- No formal report anticipated
Lockheed Missiles and Space Co. (Sunnyvale, Ca.)	1 (SN 069)	24 Dec 1976 to 5 Feb 1977	As Above/7 Hz	LMSC A/D and V/F Con- verter HP2100 or Intellec 8	LMSC Test Piers	LMSC Test report

110727

## V. SUMMARY AND COMPARISON OF TEST RESULTS BY FACILITY

Teledyne provided two SDG-5 gyros and associated test equipment to the Holloman AFB-CIGTF for evaluation as part of the HAARS testing program. Only S/N 069 was evaluated due to schedule constraints. The data acquisition system, filtering employed, test equipment and data reduction techniques are well described in [1] and are, therefore, not discussed herein. Figures 8, 9 and 10 present typical PSD gyro outputs in (DEG/HR)<sup>2</sup>/Hz for the gyro evaluated. These data provide a high confidence PSD signature for the unit evaluated over the frequency range .0001 Hz to approximately 2.5 Hz.

As equipment specifications for hardware (e.g. DRIRU II) sometimes specify the gyro output noise limits in <sup>o</sup>/HR RMS over a specific frequency range, the noise characteristic for the SDG-5 gyro was measured in appropriate units by the Martin-Marietta Corporation. Table 5 presents a comparison of the measured SDG-5 output in <sup>o</sup>/HR RMS versus the DRIRU II specification.

Data as available from the other test facilities are presented in Table 6 for comparison purposes. The data from Holloman CIGTF and the Martin-Marietta Corporation is seen to correlate reasonably well in the frequency band of .001 Hz to 5 Hz.

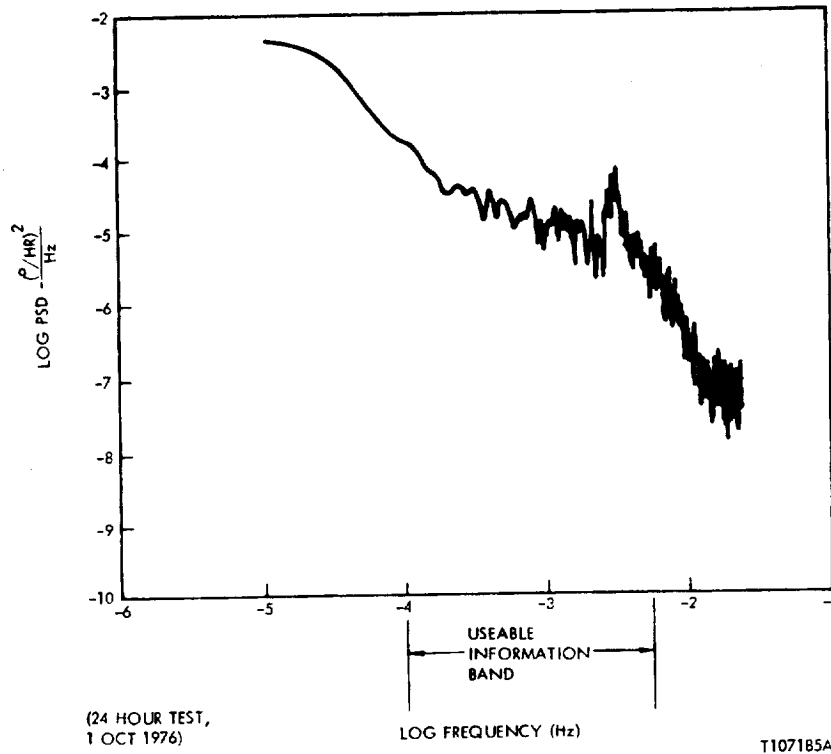


Figure 8. Power Spectral Density Gyro Output of Teledyne SDG-5 S/N 069 (Data Courtesy of Holloman AFB-CIGTF) [8]

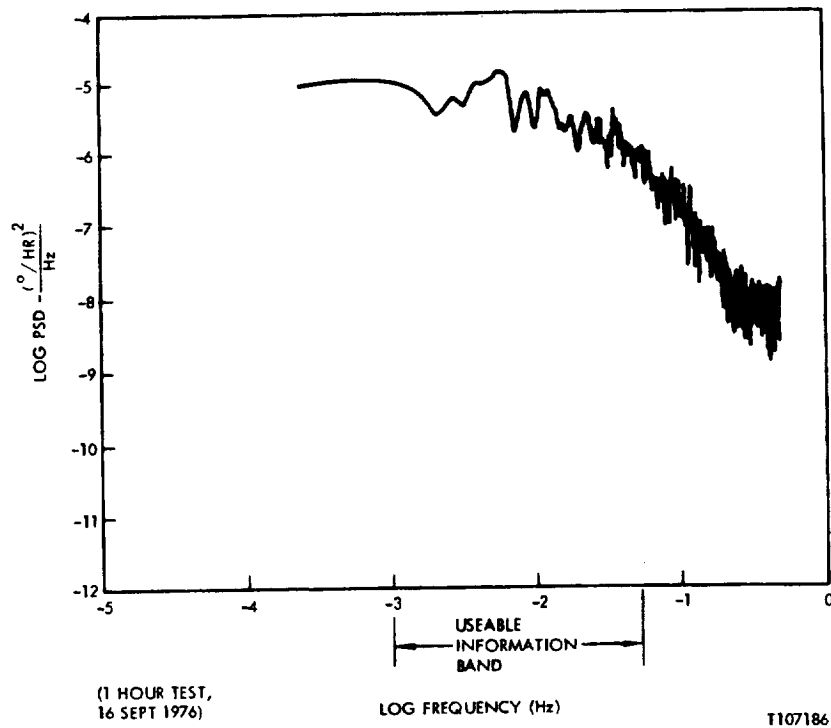


Figure 9. Power Spectral Density Gyro Output of Teledyne SDG-5 S/N 069 (Data Courtesy of Holloman AFB-CIGTF) [8]

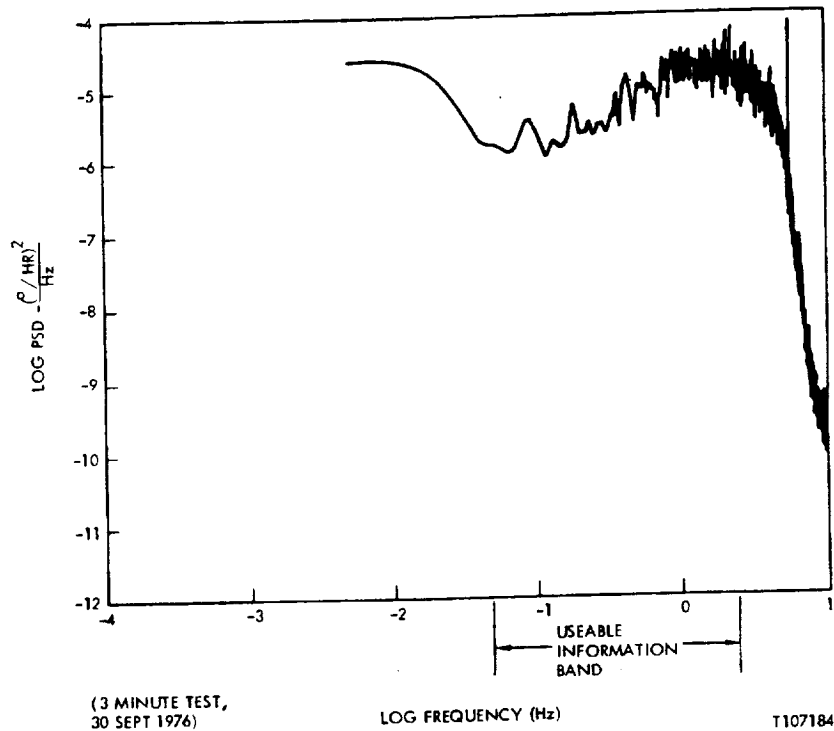


Figure 10. Power Spectral Density Gyro Output of Teledyne SDG-5 S/N 069 (Data Courtesy of Holloman AFB-CIGTF) [8]

Table 5. Comparison of Measured SDG-5 Output In ( $^{\circ}$ /Hr RMS) vs DRIRU II Specification (Data Courtesy of Martin-Marietta Corp - Denver, Co)

Frequency Range (Hertz)	Performance in $^{\circ}$ /Hr RMS		
	Axis	DRIRU II Specification	SDG-5 Performance
.01-1.0	X	.05 Max.	.004
	Y		.0032
.01-7.0	X	.5 Max.	.029
	Y		.028

Table 6. Inter Facility Comparison of PSD Test Results on Teledyne SDG-5 Gyro

Facility	Measured Gyro Noise Over Frequency (Hz) in $(g \text{ Hr})^2 / \text{Hz}$				
	.0001-.001	.001-.01	.01-.1	.1-1	1-5
Boeing Aerospace Co.	Not Measured	Not Measured	Not Measured	$2 \times 10^{-4}$ *	$1 \times 10^{-4}$
Martin-Marietta Corp.	Not Measured	$7 \times 10^{-5}$	$2 \times 10^{-5}$	$5 \times 10^{-6}$	$5 \times 10^{-5}$
Holloman CIGTF	$6 \times 10^{-5}$	$1 \times 10^{-5}$	$1 \times 10^{-6}$	$7 \times 10^{-6}$	$2 \times 10^{-5}$
Lockheed Missiles and Space Co.	Not Measured	Not Measured	$3 \times 10^{-5}$	$2 \times 10^{-5}$	$2 \times 10^{-4}$

NOTE:

SDG-5 S/N 069, SAV, axis being tested east or west was used for this comparison at the first three facilities listed above. SDG-5 S/N 036 was evaluated by Lockheed Missiles and Space Co.

\*Possible aliasing problem in data acquisition system due to incorrect filtering availability at time of test.

## VI. COMPARISON OF PSD CHARACTERISTICS OF SDG-5 DRY TDF AND SDF FLOATED GYROS

A comparison of the noise characteristics between the Teledyne SDG-5 dry TDF gyro with data for floated SDF gyros as reported in [4] was made. For convenience in making this comparison, the units of  $(\text{arc-sec})^2/\text{Hz}$  were used. A graphical presentation of this comparison is presented in Figure 11. The reader is cautioned that the sample size (one or two units) is small and that the data presented for dry TDF gyros is limited to the Teledyne SDG-5. Nonetheless, it appears that the dry-tuned ball bearing gyro performance compares quite favorably in the bandwidth of .01 Hz to approximately 5 Hz with currently used floated standards used in low jitter attitude stabilization and precision pointing systems.

## VII. METHODS FOR FURTHER NOISE REDUCTION IN DRY TUNED GYROS

The dry tuned gyro has a number of characteristic features that provide for implementing several methods for noise reduction to even lower levels than determined in the previously described testing. These consist of basic optimization of physical design parameters as briefly outlined in the following discussion.

### Physical Increase in Angular Momentum

The angular momentum of the dry gyro can be increased by adding mass to the rotor while maintaining the same spin speed with the attendant decrease in torque generator scale factor. A factor of two increase in angular momentum is readily attainable in the SDG-5. The reduction in scale factor ( $160^\circ/\text{Hr}/\text{ma}$  for SDG-5) to one-half ( $80^\circ/\text{Hr}/\text{ma}$ ) is quite acceptable for most pointing applications where maximum rate is limited to approximately  $\pm 50^\circ/\text{sec}$ . Teledyne has produced gyros (the SDG-3B) with  $2 \times 10^6$  cgs units angular momentum in lieu of  $1 \times 10^6$  cgs units for the SDG-5. Figures 12 and 13 make the comparison of key characteristics.

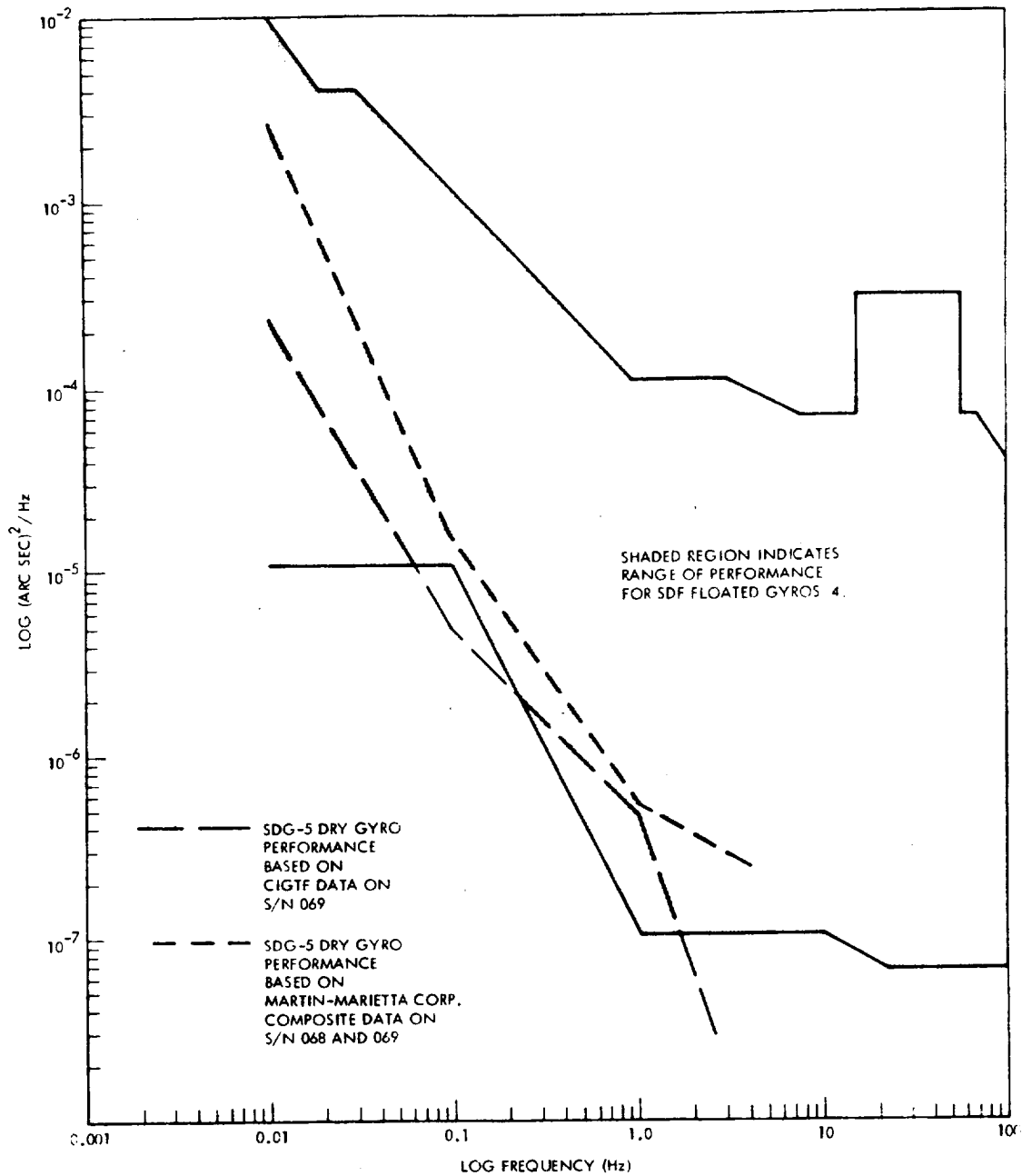
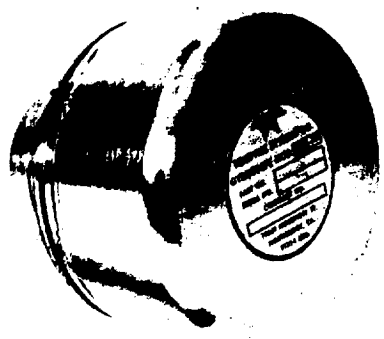


Figure 11. Graphical Comparison of Noise Characteristics in  $(\text{arc sec})^2/\text{Hz}$  for Teledyne SDG-5 Dry TDF Gyro with Floated SDF Gyros [4]

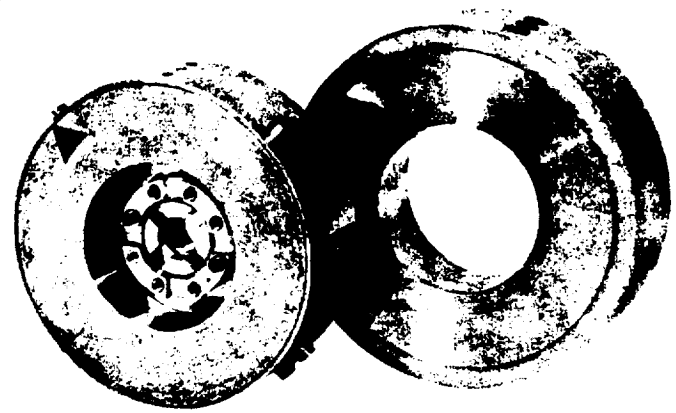


ORIGINAL PAGE IS  
OF POOR QUALITY



SDG-3B

P97177



SDG-5 ROTOR AND SDG-3B ROTOR  
(FOR COMPARISON)

P97187

Figure 12. Photograph of SDG-3B Gyroscope

APPLICATIONS		
Shipboard Inertial Navigation		
Spacecraft Guidance and Control, Fine Pointing		
Requirements for very Low Drift Rates, Low Noise and with Moderate Rate Inputs		
SPECIFICATIONS		
	<u>SDG-3B</u>	<u>SDG-5</u> (for comparison)
Size	3.25" dia x 3" long	3.0" dia x 3" long
Weight	2.9 lbs	2.3 lbs
Random drift (1σ) (Spec)	<.0005°/hr	<.001°/hr
Repeatability (day to day) 1σ - (Spec)	<.005°/hr	<.01°/hr
Angular momentum (H)	2 x 10 <sup>6</sup> CGS units	1 x 10 <sup>6</sup> CGS units
Spin speed	6000 RPM	6000 RPM

Figure 13. SDG 3B Gyro Characteristics

### Increase In Gyro Figure-of-Merit ( $F_m$ )

If one considers a figure of merit for the elastically supported gyro as defined by [9] as follows

$$F_m = \frac{C + \sum_1^n A_n}{\sum_1^n (A_n + B_n - C_n)}$$

where:

$C$  = principal moment of inertia of the rotor about the Z or spin axis

$A_n, B_n, C_n$  = principal moments of inertia of the nth gimbal about the  $X_n, Y_n, Z_n$  axes respectively

$n$  = number of gimbals

it can be shown that the  $F_m$  is approximately inversely proportional to the number of gimbals employed. This  $F_m$  for the standard SDG-5 three-gimbal gyro is 320 and can be increased to approximately 1000 by reducing the number of gimbals from 3 to 1. There is an attendant reduction in environmental "g-capability" by approximately 3 and some potential increase in 2N angular sensitivity. Teledyne has produced a small quantity of 1-gimbal units that have demonstrated extremely low random drift characteristics. No attempt to measure PSD for the 1-gimbal configuration has been made to date. This area is recommended for future investigation and evaluation for applications with relatively low environments requirements.

### Mechanization of Gimbal Angle Pickoffs

The dry gyro lends itself to incorporation of an additional instrument angle pickoff which measures the angular motion of the gimbal with respect to the case. This mechanization has been shown by [3] to provide a signal which may be used to directly compensate for "noise". As a natural consequence, a highly accurate rotor angular nulling signal, independent of the usual pickoff mechanical instability or creep is automatically provided. To the extent that the undesired shaft-to-case motion is inducing the gyro output noise, the power spectral density of this noise may be reduced by compensation by a factor which is determined essentially by the total

mechanization scale factor error. If this error is assumed to be on the order of 1.5%, as is readily achievable, then a reduction of the basic gyro output noise spectral noise by a factor of 0.015 could be realized. Teledyne is currently developing under contract from the USAF-AFAL/FDI an instrument called the Spin Coupled Accelerometer Gyro (SCAG) which is equipped with both rotor-to-case and gimbal-to-case angle pickoffs. The instrument has the necessary output information to effect the angular rate noise compensation as discussed by [3].

This same gimbal angle pickoff concept has been considered for incorporation in the SDG-5 and appears attractive.

### VIII. SUMMARY AND CONCLUSIONS

The following conclusions are made based on the foregoing data and discussions:

1. The SDG-5 gyro output noise power spectral density characteristics have been determined to a high confidence level in the frequency band of .001 Hz to 5 Hz by the testing accomplished to date.
2. The SDG-5 is an excellent candidate gyro for fine pointing applications where low noise performance below 1 Hz are specified in milliarc-seconds and that operate with control system bandwidths in the region of 1 Hz.
3. The SDG-5 PSD performance compares quite favorable with currently used SDF floated gyros below 1 Hz and from 1 Hz to 10 Hz the SDG-5 performance compares midrange with other state-of-the-art precision gyroscopes.
4. A number of attractive methods for effecting a further decrease in the SDG-5 noise characteristics are readily available and should be pursued.

### IX. ACKNOWLEDGEMENTS

The authors wish to express their gratitude to the following organizations for their cooperation in conducting the reported testing in a demanding schedule environment and on an as equipment/gyro availability basis:

The Martin-Marietta Corporation  
Holloman AFB-CIGTF  
The Boeing Aerospace Company  
The Lockheed Missiles and Space Company

## REFERENCES

- [1] Price, Craig H., Gyro Noise Testing in the Low Frequency Range Using PSD Analysis. Paper presented at the AIAA Guidance and Control Conference, San Diego, California/August 16-18, 1976.
- [2] Gates, R. L., Testing Technology for Fine Pointing Systems, Paper presented at the Seventh Biennial Guidance Test Symposium, Holloman AFB, New Mexico/ May 14-16, 1975.
- [3] Erdley, H. F., Teledyne Low Noise Gyro. Teledyne Technical Report dated July 1976.
- [4] Truncale, A, Koenigsberg, W. and Harris, R., Spectral Density Measurements of Gyro Noise. Charles Stark Draper Laboratory Report E-2641, February 1972.
- [5] Gates, R. L., Evaluation of Noise Characteristics of the Teledyne SDG-5 Gyroscope for Fine Pointing Applications. Martin-Marietta Corporation Proprietary Report
- [6] Teledyne Document 50317, Description and Operating Instructions for the Teledyne Strapdown Gyro Laboratory Test Equipment, September 1976.
- [7] Strapdown Gyro - Description and Performance Data Summary. Teledyne Systems Company, January 1976.
- [8] The Teledyne SDG-5 Gyro Test - Performed by the 6585th Test Group, Holloman Air Force Base - CIGTF, Report No. TBD, February 1977
- [9] Craig, Robert J.G., Theory of Errors of a Multigimbal, Elastically Supported, Tuned Gyroscope. IEEE Transactions on Aerospace and Electronic Systems, Vol. AES, No. 3, May 1972.

APPENDIX B

FIRST-DIFFERENCE PERFORMANCE DATA ON  
TELEDYNE SDG-5 GYRO



# MEMORANDUM

NO: RBI/3082

DATE: 18 April 1977

TO: Distribution  
FROM: R. Irvine ✓  
SUBJECT: First-Difference Performance Data on  
Teledyne SDG-5 Gyro  
REFERENCE:

---

The subject attached data (Attachment 1) was taken on Gyro Serial Number 069 at the Martin Marietta Corporation - Denver. This data essentially shows the RMS drift performance as a function of sample interval. It is also a good measure for judging the gyro performance in terms of gyro-compass quality.

Attachment 2 describes the data reduction technique and provides some additional interpretation.

  
R. B. Irvine

RBI/ams

## Attachments

1. First-Difference Data, Teledyne Gyro. Inter-Department Communication, Martin Marietta Aerospace, dated 15 March 1977.
2. AIAA Paper No. 70-1012, TRIM-A Gyromonitor IMU Incorporating the Gyroflex Gyro, Robert L. Gates, 17-19 August 1970.

## Distribution

D. Eller	H. Halamandaris
SDG-5 File	A. Schmitt
J. Dowell	R. VanAlstine
S. Kinsinger	L. Krieger
P. Donoghue	K. Green
L. Cotter	J. Ritter
F. McNair	G. Nappus
H. Erdley	T. Wirt
D. Doty	G. Wunder

ATTACHMENT 1

INTER-DEPARTMENT COMMUNICATION

MARTIN MARIETTA AEROSPACE

15 March 1977  
77-JT-0510-30

To: N. Osborne  
cc: R. L. Gates  
From: J. Tietz  
Subject: First-Difference Data, Teledyne Gyro

-----

First-difference drift tests have been completed on the Teledyne gyro, ID number D007013. These tests were done at the Martin Marietta Inertial Guidance Laboratory under IRAD task 48641. The test configuration used and the test results are shown below.

Sample Interval (seconds)	First Difference (RMS, Degrees/Hour)			
	Input Axis East-West	Data File	Input Axis North-South	Data File
.1	.0376	TD219F	.0488	TD210F
1.	.00425	TD218F	.00504	TD211F
10.	.000761	TD217F	.000786	TD212F
100.	.000235	TD216F	.000268	TD213F
1000.	.000104	TD215F	.000120	TD214F

TABLE 1. TEST RESULTS

15 March 1977

77-JT-0510-30

Page 2

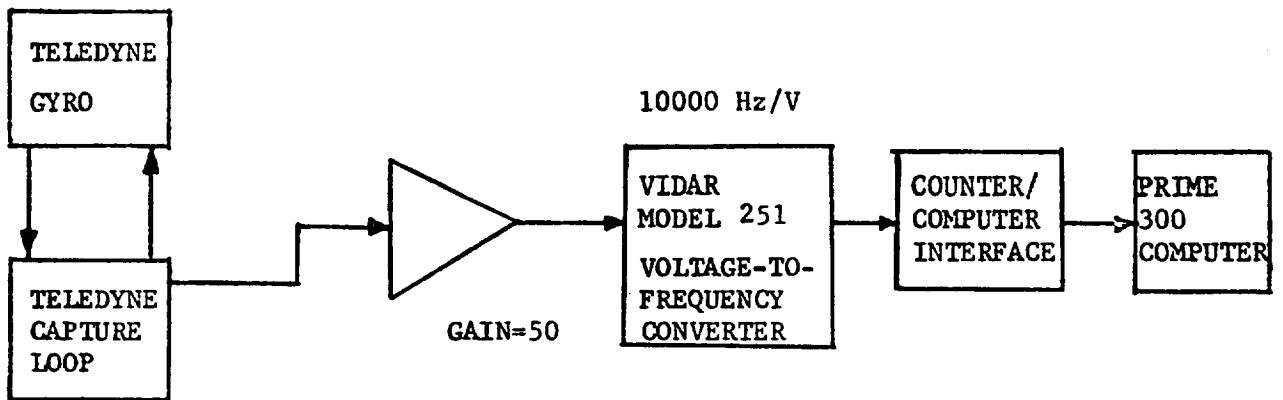


FIGURE 1. TEST CONFIGURATION

*John C Tietz*  
John Tietz  
Guidance & Controls  
Inertial Guidance Laboratory

64



ORIGINAL PAGE IS  
OF POOR QUALITY

Preceding page blank

B5

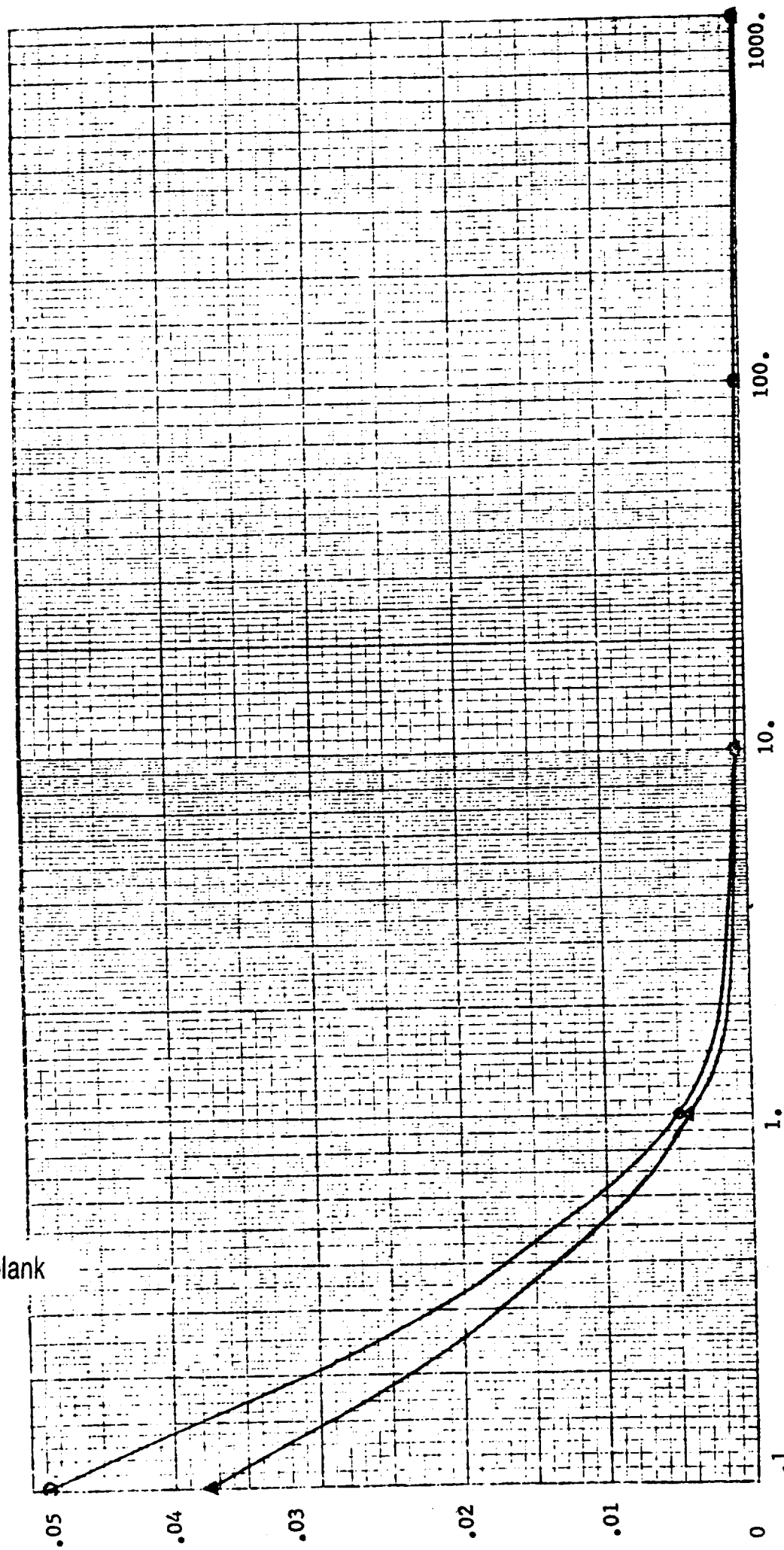
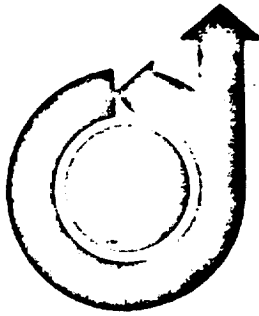


FIGURE 2. FIRST DIFFERENCE VS SAMPLE INTERVAL



**AIAA Paper  
No. 70-1012**

**TRIM— A GYROMONITOR IMU INCORPORATING THE GYROFLEX GYRO**

by  
**ROBERT L. GATES**  
Singer-General Precision, Incorporated  
Little Falls, New Jersey

# **AIAA Guidance, Control and Flight Mechanics Conference**

**SANTA BARBARA, CALIFORNIA/AUGUST 17-19, 1970**

First publication rights reserved by American Institute of Aeronautics and Astronautics,  
1290 Avenue of the Americas, New York, N. Y. 10019. Abstracts may be published without  
permission if credit is given to author and to AIAA. (Price: AIAA Member \$1.25. Nonmember \$2.00).

Note: This paper available at AIAA New York office for six months;  
thereafter, photoprint copies are available at photocopy prices from:  
Technical Information Service, 750 3rd Ave., New York, N.Y. 10017

B6

-- NOTES --



# TRIM - A GYROMONITOR IMU INCORPORATING THE GYROFLEX<sup>®</sup> GYRO

Robert L. Gates  
Senior Staff Member  
Singer-General Precision, Inc.  
Kearfott Division  
Little Falls, New Jersey

## Abstract

The concept and theory of operation of a self-calibrating gyromonitor inertial measurement unit is described. The mechanization utilizes the redundant axis of the azimuth gyro as the measurement axis to obviate the need for an additional gyroscope. An experimental model of the platform using the GYROFLEX Gyro is described and test instrumentation and test data are presented. Performance predictions are made in terms of cruise navigation accuracy showing the improvements possible with reduction of uncertainty gyro drift. Also discussed are the advantages of explicit in-flight gyro calibration in terms of confidence in the accuracy of a pure inertial navigator.

## I. Introduction

The concept and theory of operation of an experimental gyromonitor inertial measurement unit is presented; the end product should be particularly suited for cruise type applications. Some interesting aspects of navigation systems incorporating this concept are as follows:

1. Rapid, self-contained azimuth\* gyro calibration is possible for a pure inertial navigation (only method known to the author).
2. Gyromonitoring is accomplished without the requirement for a redundant instrument. The azimuth gyro redundant axis is used in a mechanization described further on.
3. The TRIM concept may dissolve up to 90% of the "dead reckoning" associated with a pure inertial navigator.

Experimental test data have been obtained which indicate solid potential for achieving gyro performance for an unaided inertial navigator in the .002 to .005 %/hr - one sigma - range. This performance is compatible with better than 0.5 nm/hr performance.

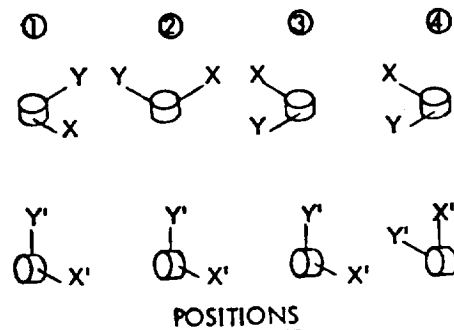
## II. Theory of Operation

The basic idea is a simple one which takes advantage of the normally unused redundant axis of the platform azimuth gyro that is present when two-degree-of-freedom gyros are used in the platform. The platform cluster is constructed by mounting the gyros in turntable modules that permit the gyros to be independently repositioned at the cardinal angles. The case rotations are made around the gyro spin axes. During rotations, signal resolvers direct the gyro outputs to the proper gimbal axes. The gyros are not torqued during the slew interval.

\*In Avionics terminology, the "azimuth" gyro is the one of the orthogonal set which controls the stable member around the vertical axis. The "vertical" gyro has its input axes in the horizontal plane.

The self-calibration is accomplished by taking simultaneous samples of gyro command and capture signals for the two parallel gyro input axes (see position ① of the sketch below), one of which is always the azimuth gyro rate captured redundant axis and the other will be one of the two axes of the vertical gyro. Summing or differencing of the simultaneous measurements permits implicit cancellation of platform inertial rate (known or unknown) around the monitor axis thereby permitting operation on a fixed or moving base (aircraft carrier or airborne). This is the well known principle of the gyromonitor. (3,4,5,6)

The gyro drift coefficients are recovered from a set of samples\*\* (such as data from relative positions ① and ③, see sketch below). The accelerometers are not required in the measurement loops and do not contribute error. The four relative gyro positions are shown below. Positions ①, ②, and ③ are required for data acquisition and are achieved by sequentially indexing the vertical gyro. Position ④ places the calibrated azimuth gyro X' axis into the azimuth position completing one calibration cycle. Note that X' is the redundant axis for relative positions ①, ②, and ③ and that Y' is the redundant rate axis in position ④.



This capsule description indicates how gyromonitoring is feasible without a redundant gyro. Also apparent is the very simple but important idea of periodically replacing the uncalibrated azimuth axis with an axis of the same gyro which has been explicitly calibrated in the horizontal plane. The redundant axis calibration does not include spin axis mass unbalance; for this reason, the unique characteristic of the GYROFLEX wherein mass unbalance stability is superior proves valuable (the spin axis bearings do not contribute to spin axis mass unbalance). (2) A laboratory model of this type of IMU is shown in Figure 1.

\*\*See Appendix A

ORIGINAL PAGE IS  
OF POOR QUALITY

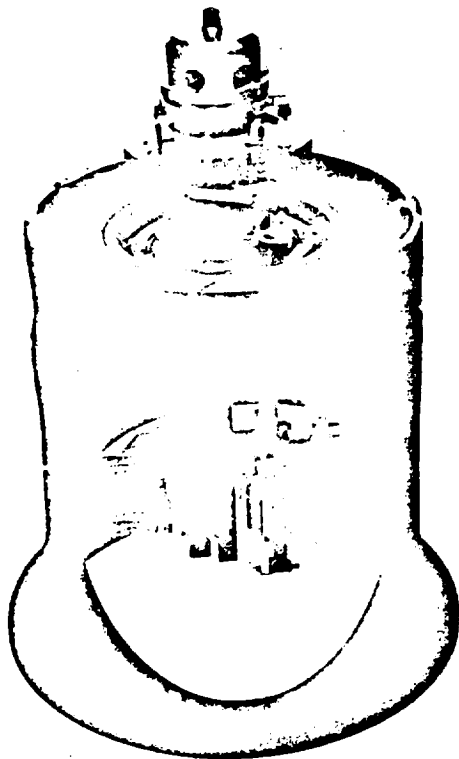


FIGURE 1. BRASSBOARD PLATFORM

### III. Performance Prediction

The iterative recovery of gyro drift coefficients strongly qualifies the use of the modern filter theory in the system software. (1) In fact, a real time history of gyro performance during the mission will be available in the system computer. When compared to standard expected coefficient variations during flight, a measure of performance quality may be determined.

For example, the first test would be to verify that the coefficient is within the  $\pm 3$  sigma limits from each coefficient mean established as the acceptable day-to-day (or on-off) performance of the gyro; these limits with the gyro-monitor mechanization can be an order-of-magnitude larger than conventional system limits (say  $\pm 0.3\%/hr$ ). The second test will be against the magnitude of change of the coefficient with each major cycle of the TRIM Mode. The Figure 2 shows a plot of actual TRIM IMU data which would be representative of changes between samples (first differences) available within the computer. The RMS value of the changes is representative of gyro performance. For this particular run, the RMS value was  $0.0038\%/hr$  based upon one-minute duration samples.

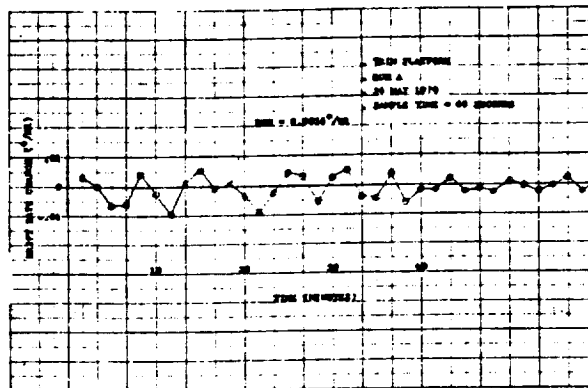


FIGURE 2. DRIFT RATE CHANGE  
BETWEEN COEFFICIENT RECOVERIES

Based upon these measurements, a real time estimate of CEP may be made using system state variables in an error analysis simulation. This CEP could be displayed for the aircraft commander or navigator thus markedly reducing the "dead reckoning" aspects of a pure inertial navigator since for most 1 mph class systems up to 90% of the error budget belongs to the system gyros.

### IV. Navigation Accuracy

A DELTA Curve for the GYROFLEX is shown in Figure 3. The concept of this method of data presentation is discussed in detail in Appendix B.

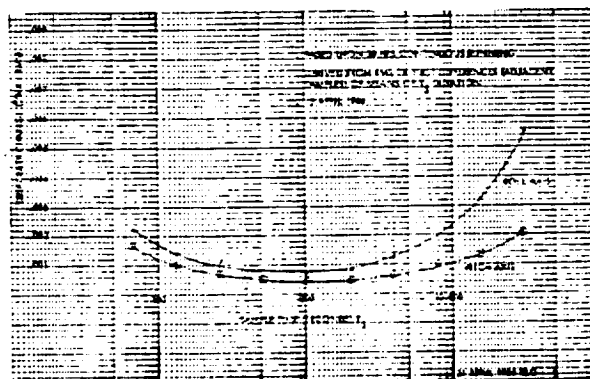


FIGURE 3. GYROMONITOR EVALUATION--  
DELTA CURVE  
SHORT-TERM PERFORMANCE - GYROFLEX SN 113

This function is obtained by computing the RMS of first differences as a function of integration time which is varied over the sample times of interest. Figure 3 is for a gyro in steady state operation. From Figure 2 we can see that the gyro contribute about  $0.0021\%/hr$  to the RMS level of  $.0038\%/hr$  at the IMU level. Figure 4 shows a drift rate ramp analytically included to simulate the warmup transient or a trending gyro.

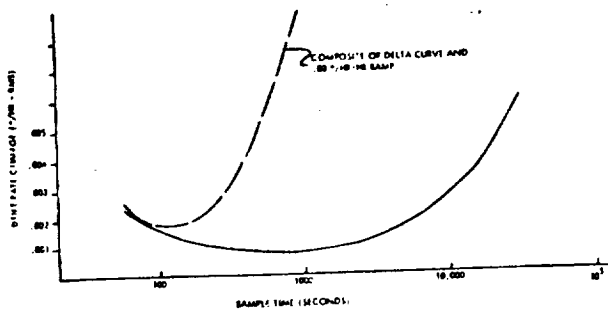


FIGURE 4. NAVIGATION GYRO IN PRESENCE OF A RAMP DRIFT

This illustrates the value of using an adaptive sample time to optimize performance. That is, sample time should be short during warmup and increase as the gyro drift reaches steady state. Figure 5 shows CEP vs gyro ramp drift rate utilizing the optimum sample time.

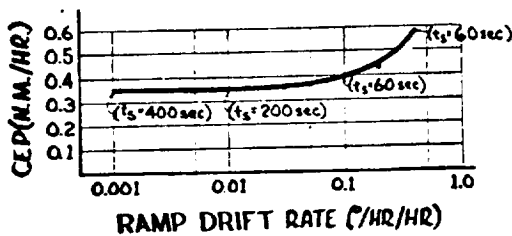


FIGURE 5. CEP vs RAMP DRIFT RATE FOR TRIM IMU (USING OPTIMUM SAMPLE TIME)

### V. IMU Comparison (Figure 6)

Some IMUs use continuous motion case rotation of the gyro or of the cluster for spatial modulation to average the effects of gyro drift (again exclusive of spin axis mass unbalance). TRIM does not depend upon spatial modulation but incorporates explicit numerical recovery of drift coefficients with computer compensation for system error.

TYPE	SELF CALIB CAPABILITY			
	CONVENTIONAL UNAIDED	CONTINUOUS CASE ROTATION	SPATIAL MODULATION	NUMERICAL RECOVERY
CONVENTIONAL UNAIDED	NO	NO	NO	NO
AUTOBIAS	NO	YES (15)	YES (11)	NO
AIDED (DOPPLER/LORAN)	YES	YES (40)	YES (12)	YES
CONTINUOUS CASE ROTATION	NO	NO	NO	YES
SDF GYROMONITOR	YES	NO	YES (105)	YES
TRIM	YES	YES (35)	YES (36)	YES

NOTE: NUMBERS IN PARENTHESES INDICATE HOURS PER CYCLE

FIGURE 6. IMU SURVEY

The standard gyromonitor system utilizing single-degree-of-freedom gyros requires forced precession of the gyro spin vector with gyro indexing. This results in the requirement for a settling time period which slows reaction time. TRIM gyro case rotations are around the spin axis and since each gyro is geometrically stabilized by the gimbal servos, the rotor must remain undisturbed with each indexing. This should permit the reduction of monitor "off time" (slew and settling time) by a factor of 3 to 7 resulting in a significantly shorter mode cycle time.

### VI. Test Results

An experimental IMU (see Figure 1) has been fabricated to investigate the performance potential of this mechanization. The hardware was intended for laboratory use and will be used for experiments in support of design tradeoffs and for feasibility demonstration. The unit is basically a multi-axis servotable. The cluster mounted turntables for indexing the gyros are derived from a gyrocompass system designated GUARD which is in production for the Air Force. Pitch, roll, and azimuth isolation axes are provided between the outer housing and the cluster for dynamic simulation of an operational IMU. A support electronics console is used to provide power supplies, gyro and accelerometer excitation and temperature control and capture loop circuits, gimbal servo electronics and readout instrumentation. The analog-to-digital conversion instrumentation is discussed in Appendix B. An automatic electromechanical programmer is used to cycle the system through the TRIM Mode.

### Test Objectives

A number of questions were to be answered, and experimentally verified, with respect to gyro performance and IMU performance.

1. Can the "implicit" cancellation of inertial rates common to the parallel axes be demonstrated? And, can the absolute value of the gyromonitor recovered coefficient be verified?
2. What is the accuracy and reaction time potential of the concept at the system level?
3. What is the RMS level of performance with and without filtering?
4. In a more detail sense, what are the deleterious effects, if any, of indexing the gyros?

### Test Data

The figure entitled "Implicit Noise Cancellation" (Figure 7) demonstrates two important facts. One is a confidence verification that the proper absolute value of drift coefficient is being recovered in the gyromonitor mode. The other is a demonstration of "implicit cancellation" of unknown platform rates that might be thought to interfere with the concept.

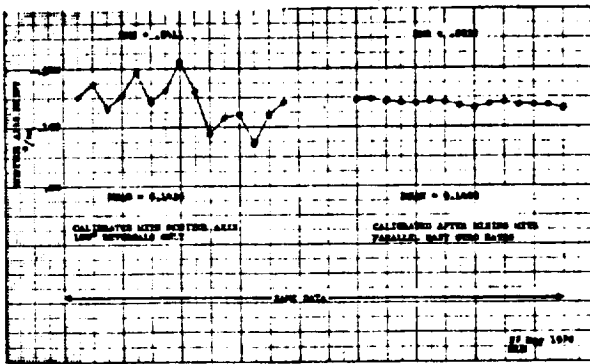


FIGURE 7. TRIM IMPLICIT NOISE CANCELLATION

The data were taken with the platform in an earth slaved mode. The redundant axis of the azimuth gyro was sequentially indexed from nominally East to nominally West (although absolute heading is immaterial to the test). At each position, simultaneous and average rate outputs were separately recorded from the redundant axis and the parallel vertical gyro axis for 60-second intervals.

The plot on the left was derived by using the redundant axis data separately to calibrate its fixed drift coefficient  $D(Y)_F$ . This was done in an analogous fashion to standard two-position gyro testing wherein one-half the sum of East and West readings yields fixed drift and earth rate coupling is cancelled. The large scatter (.149% peak-to-peak and .041% RMS) is a result of cluster motion during the short sample time.

The plot on the right is achieved by "mixing" the same redundant axis data with data from the parallel vertical gyro input axis. The simultaneous samples are alternately summed and differenced to implicitly cancel the common inertial noise rate. Note that the RMS scatter in calibrating  $D(Y)_F$  is reduced by an order-of-magnitude. Also, note the excellent agreement in the average value of  $D(Y)_F$  (difference of 0.0026%/hr) obtained by the separate methods. The parallel vertical gyro axis is calibrated simultaneously although the plot is omitted for clarity.

The figure entitled "Day-to-Day and Random Drift Error Reduction with TRIM" (Figure 8) is a clear picture of the concept value. Test data have been obtained pointing to a pure inertial navigation system accuracy of 0.35 nm/hr or better.

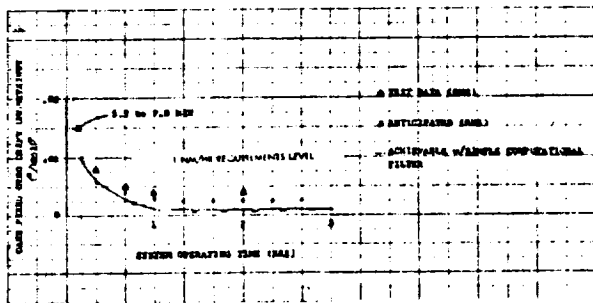


FIGURE 8. DAY-TO-DAY AND RANDOM DRIFT ERROR REDUCTION WITH TRIM

The test data points (triangles) are the results of more than 9 runs and 6 shutdowns with some 144 complete TRIM cycles comprised of either 3 or 6 indexing positions each cycle. It is anticipated that slightly better results (X plot) will be achieved in the brassboard experiment with some refinements. The curve of results with filtering should be realized when the data are reprocessed through either a minimum Kalman filter or a limited least-squares fit routine. The triangular data plots are the RMS values of first differences of adjacent coefficient recoveries.

An example of reaction time data are presented in Figure 9.

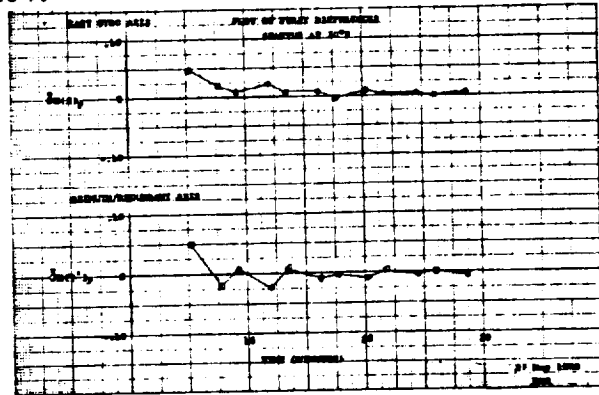


FIGURE 9. DRIFT COEFFICIENT RECOVERY DURING WARMUP

The plotted points represent the pure "unmodeled" drift coefficients plotted in terms of magnitude change between recoveries. Improved results will be obtained with a more optimum heater power distribution to the gyro and to the cluster structure. Nevertheless, the data from the 5.2 to 7.8 minute interval are accurate to 0.015%/hr.

Figure 10 presents a plot that is typical of gyro drift settling following a slew. The plot shows that the gyro recovers in about 8 seconds. These data were taken from the rate captured horizontal monitor axis of the azimuth gyro (spin axis horizontal). Therefore, for the GYROFLEX Gyro, data accumulation may begin 8 to 10 seconds following a case slew.

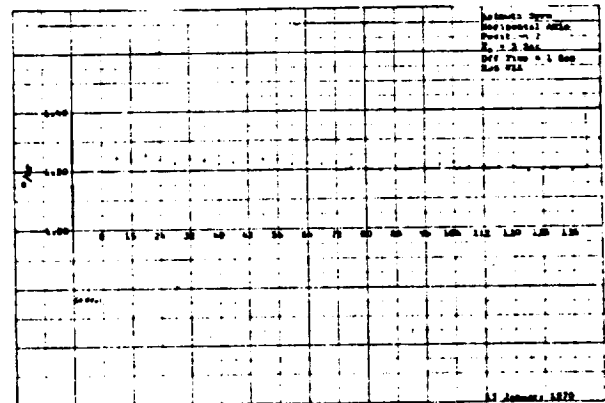


FIGURE 10. GYRO SETTLING CHARACTERISTIC



In comparing the data to other instruments, we have noted that floated single axis gyros may require 60 to 100 seconds settling time following case indexing around the output axis.

The redundant axis rate data may also be used for platform gyrocompassing, or in a more exact sense, heading determination. With the cluster leveled in a conventional leveling mode and earth slaved in azimuth, the redundant axis will sense a component of horizontal earth rate proportional to the deviation of the azimuth gyro spin axis from the meridian plane. This is true at the 0° and 180° positions. Heading may be determined by differencing the two measurements and solving for the heading angle (fixed drift D(X)† is implicitly cancelled).

$$\psi = \frac{\omega_{0^{\circ}} - \omega_{180^{\circ}}}{2\Omega \cos \lambda}$$

For repetitive heading determinations, the non-repeatability or random error will be primarily a function of fixed drift change between samples. Figure 11 shows the results of a run where the heading determinations are plotted.

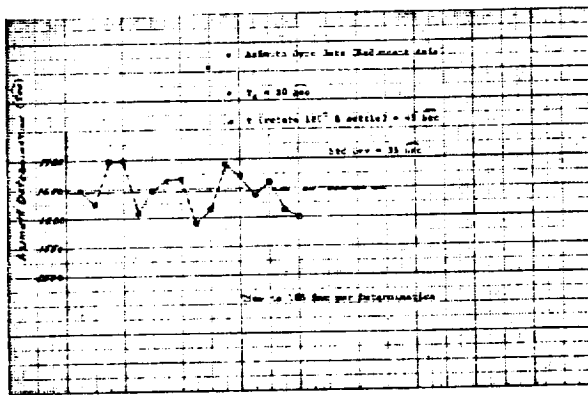


FIGURE 11. TRIM GYROCOMPASS DATA

Note that the platform had a mean heading of 1645 arc seconds and that the standard deviation for 16 individual determinations was 35 arc seconds. In this case, the gyro was in thermal steady state and the sample time was reduced to 30 seconds.

#### References

- (1) Carlstrom, R., Gold, E., Reilly, A., "INS-A Marine Stellar-Inertial System with Optimum DATA Processing", Conference Proceedings, AIAA/JACC Guidance and Control Conference, August 15-17, 1966
- (2) Cimera, R., Napolitano, M., "The GYROFLEX Gyro-scope--An Unconventional Inertial Sensor", Conference Proceedings, Symposium on Unconventional Inertial Sensors, Vol. 1, December 1966
- (3) Gates, R. L., "The Fourth Gyro", GPI, TNB, Vol. 7, No. 4, 4th Quarter 1964
- (4) Griffin, R. E., "Improved Navigation Accuracy with the Gyro Monitor", Conference Proceedings, 1964 IEEE 8th International Convention on Military Electronics, September 14-16, 1964

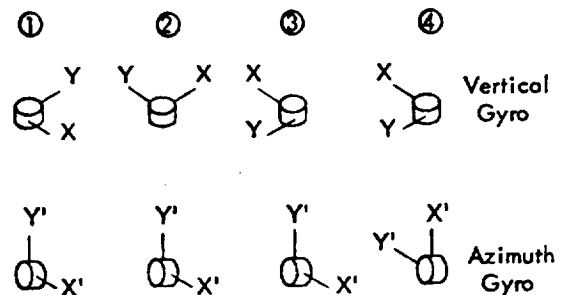
- (5) Lee, B., "The Improvement of a Low-Cost Inertial Navigator Through Conditional Feedback", IEEE Transactions on Aerospace and Electronic Systems, Vol. AES-4, No. 4, July 1968
- (6) Rosen, L. L., "Concepts of Gyro Monitoring as Applied to Long Term Inertial Navigation", Conference Proceedings, 1964 IEEE 8th International Convention on Military Electronics, September 14-16, 1964

## APPENDIX A

### TRIM-IMU Functional Equations With Gyro Error Model

#### Introduction

This section derives and presents the basic functional equations for navigation computer recovery of the vertical and azimuth gyro drift coefficients (bias values) for a trim GYROFLEX Gyro platform mechanized for the TRIM gyro-monitor mode. The implicit cancellation of some drift terms and platform command rates are presented in the derivation. The four relative gyro positions are shown below.



POSITIONS

#### Derivation - TRIM MODE

The gyromonitor equations may be derived by considering the inertial angular rates and the drift rates† of the gyro pair with respect to a reference inertial coordinate frame XYZ. Consider first the rates  $\Omega$  for the navigation (N) gyro vertical X axis with respect to the reference frame.

Navigation Gyro, (X axis, position ①)

$$\Omega_{XN} = -\omega_{XC} + D(X)_T$$

where,

$\omega_{XC}$  = command rate to X axis of vertical gyro which can be expressed as  $S_{YN}^i \dot{Y}_N$

$D(X)_T$  =  $D(X)_F + D(X)_{S\alpha_S} + D(X)_{SS\alpha_S}^2$  and hence contains the total for the vertical gyro ( $\alpha_S$  is 1 g acceleration along the spin axis).

further,

$D(X)_F$  = gyro drift (%/hr) about the X axis which is insensitive to acceleration.

† See general GYROFLEX error model in latter part of this

$D(X)_S$  = gyro drift ( $^{\circ}/hr/g$ ) about the X axis attributable to acceleration ( $a_S$ ) along the spin axis.

$D(X)_{SS}$  = gyro drift ( $^{\circ}/hr/g^2$ ) about the X axis attributable to acceleration squared ( $a_S^2$ ) along the spin axis.

$S_{YN}^i YN$  = the product of Y axis torquer scale factor ( $^{\circ}/hr/ma$ ) and the average value of the command current (ma) for the vertical gyro navigation (N) axis.

so,

$$S_{YN}^i YN = -\Omega_{XN} + D(X)_T \quad (A)$$

Likewise, for the monitor axis,

$$\Omega_{XM} = -\Omega_{XN} + D(X)' + D(X)'_Y a_Y$$

As a rate captured axis,  $\Omega_{XM}$  is analogous to the capture rate  $S_{YM}^i YM$  hence,

$$S_{YM}^i YM = -\Omega_{XN} + D(X)'_F + D(X)'_Y a_Y \quad (B)$$

Simultaneous differencing of equations (A) and (B) permits implicit cancellation of the inertial rate term  $\Omega_{XN}$  and the residual contains the drift coefficients of interest.

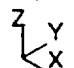
$$S_{YM}^i YM - S_{YN}^i YN = D(X)'_F + D(X)'_Y a_Y - D(X)_T$$

A more practical approach from the mechanization viewpoint in the presence of noise and disturbance inputs, is to consider differencing the average or fitted values of the terms on the left side for a finite sample interval (say 20 to 100 seconds duration) in each measurement position designated by the symbol  $\textcircled{1}$ .

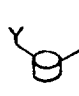
$$(S_{YM}^i YM - S_{YN}^i YN)_{\textcircled{1}} = D(X)'_F + D(X)'_Y a_Y - D(X)_T \quad (C)$$

#### Navigation Gyro (Y axis, position $\textcircled{2}$ )

Similarly, the equations are derived for position and sample  $\textcircled{2}$ , this time involving the navigation gyro Y axis.



$$\Omega_{XN} = -\omega_{YC} - D(Y)_T$$



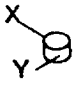
$$S_{XN}^i XN = -\Omega_{XN} - D(Y)_T \quad (D)$$

Equation (B) still applies for the monitor axis since its attitude is unchanged with respect to the reference frame. Similarly, inspection of equations (B) and (D) reveals that the inertial rate for the new position/sample interval  $\textcircled{2}$  may be cancelled by differencing, i.e.,

$$(S_{YM}^i YM - S_{XN}^i XN)_{\textcircled{2}} = D(X)'_F + D(X)'_Y a_Y + D(Y)_T \quad (E)$$

#### Navigation Gyro (X axis, position $\textcircled{3}$ )

This position places the navigation gyro X axis  $180^{\circ}$  from the first set (sample  $\textcircled{1}$ ).



$$\Omega_{XN} = \omega_{XC} - D(X)_T$$

which becomes

$$S_{YN}^i YN = \Omega_{XN} + D(X)_T \quad (F)$$

Equation (F) is summed with the monitor equation (B) for position/sample interval  $\textcircled{1}$ :

$$(S_{YM}^i YM + S_{YN}^i YN)_{\textcircled{1}} = D(X)' + D(X)'_Y a_Y + D(X)_T \quad (G)$$

The vertical gyro X axis drift may then be explicitly recovered by subtracting equation (C) from equation (G).

$$D(X)_T = \frac{1}{2} (S_{YM}^i YM + S_{YN}^i YN)_{\textcircled{1}} - \frac{1}{2} (S_{YM}^i YM - S_{YN}^i YN)_{\textcircled{1}} \quad (H)$$

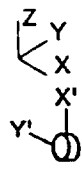
Likewise, the equations associated with positions  $\textcircled{1}$ ,  $\textcircled{2}$ , and  $\textcircled{3}$  may be combined to recover  $D(Y)_T$  to complete vertical gyro calibration.

$$D(Y)_T = S_{YM}^i YM - S_{XN}^i XN - \frac{1}{2} (S_{YM}^i YM - S_{YN}^i YN)_{\textcircled{1}} - \frac{1}{2} (S_{YM}^i YM + S_{YN}^i YN)_{\textcircled{3}} \quad (I)$$

The fixed drift of the azimuth gyromonitor axis X' is also recoverable.

$$D(X)' = \frac{1}{2} (S_{YM}^i YM - S_{YN}^i YN)_{\textcircled{1}} + \frac{1}{2} (S_{YM}^i YM + S_{YN}^i YN)_{\textcircled{3}} - D(X)'_Y a_Y \quad (J)$$

The so-called "quadrature g" term  $D(X)'_Y$  is present because of the presence of 1 g along the azimuth axis and is included for completeness. If truly measurable, this term will be "tagged" at the component level and the computer will remove its contribution. This term does not effect a conventional IMU.

 The azimuth gyro is now rotated to position  $\textcircled{4}$  thereby completing the first calibration cycle. Azimuth gyro drift around the new gyro axis may be written as:

$$\Omega_Z = D(X)' - D(X)'_X a_X + D(X)'_{XX} a_X^2$$

All significant drift terms are now known. The fixed drift coefficient  $D(X)'$  was recovered from equation (J) above. The spin axis mass unbalance term  $D(X)'_X$  is a computer stored coefficient available from factory or periodic calibration. Present indications are that the g squared coefficient  $D(X)'_{XX}$  is negligibly small.

#### Holloman GYROFLEX Error Model

The performance model assumed for the GYROFLEX is:

$$S_{TGY}^i Y = D(X)'_F + D(X)'_X a_X + D(X)'_Y a_Y + D(X)'_S a_S + D(X)'_{XX} a_X^2 + D(X)'_{SS} a_S^2 + D(X)'_{XY} a_X a_Y + D(X)'_{XS} a_X a_S + D(X)'_{YS} a_Y a_S - \omega_X$$

$$S_{TGX}^i X = D(Y)'_F + D(Y)'_Y a_Y + D(Y)'_X a_X + D(Y)'_S a_S + D(Y)'_{YY} a_Y^2 + D(Y)'_{SS} a_S^2 + D(Y)'_{YX} a_Y a_X + D(Y)'_{YS} a_Y a_S + D(Y)'_{XS} a_X a_S + \omega_Y$$

where  $\vec{X} \times \vec{Y} = \vec{S}$

Definition of Performance Model Terms

$i_Y$	current flow through the Y axis torque generator (ma)
$S_{TGY}$	sensitivity of the Y axis torque generator ( $^{\circ}/hr/ma$ )
$i_X$	current flow through the X axis torque generator (ma)
$S_{TGX}$	sensitivity of the X axis torque generator ( $^{\circ}/hr/ma$ )
$a_X$	acceleration along the X axis (g)
$a_Y$	acceleration along the Y axis (g)
$a_S$	acceleration along the spin axis (g)
$D(X)_F$	gyro drift ( $^{\circ}/hr$ ) about the X axis which is insensitive to acceleration
$D(Y)_F$	gyro drift ( $^{\circ}/hr$ ) about the Y axis which is insensitive to acceleration
$D(X)_{X^aX}$	gyro drift ( $^{\circ}/hr$ ) about the X axis attributable to acceleration along the X axis, where $D(X)_X$ ( $^{\circ}/hr/g$ ) is a drift coefficient
$D(Y)_{Y^aY}$	gyro drift ( $^{\circ}/hr$ ) about the Y axis attributable to acceleration along the Y axis, where $D(Y)_Y$ ( $^{\circ}/hr/g$ ) is a drift coefficient
$D(X)_{Y^aY}$	gyro drift ( $^{\circ}/hr$ ) about the X axis attributable to acceleration along the Y axis, where $D(X)_Y$ ( $^{\circ}/hr/g$ ) is a drift coefficient
$D(Y)_{X^aX}$	gyro drift ( $^{\circ}/hr$ ) about the Y axis attributable to acceleration along the X axis, where $D(Y)_X$ ( $^{\circ}/hr/g$ ) is a drift coefficient
$D(X)_{S^aS}$	gyro drift ( $^{\circ}/hr$ ) about the X axis attributable to acceleration along the spin axis, where $D(X)_S$ ( $^{\circ}/hr/g$ ) is a drift coefficient
$D(Y)_{S^aS}$	gyro drift ( $^{\circ}/hr$ ) about the Y axis attributable to acceleration along the spin axis, where $D(Y)_S$ ( $^{\circ}/hr/g$ ) is a drift coefficient
$D(X)_{XX^a2}$	gyro drift ( $^{\circ}/hr$ ) about the X axis attributable to the square of acceleration along the X axis, where $D(X)_{XX}$ ( $^{\circ}/hr/g^2$ ) is a drift coefficient
$D(Y)_{YY^a2}$	gyro drift ( $^{\circ}/hr$ ) about the Y axis attributable to the square of acceleration along the Y axis, where $D(Y)_{YY}$ ( $^{\circ}/hr/g^2$ ) is a drift coefficient
$D(X)_{SS^a2}$	gyro drift ( $^{\circ}/hr$ ) about the X axis attributable to the square of acceleration along the spin axis, where $D(X)_{SS}$ ( $^{\circ}/hr/g^2$ ) is a drift coefficient
$D(Y)_{SS^a2}$	gyro drift ( $^{\circ}/hr$ ) about the Y axis attributable to the square of acceleration along the spin axis, where $D(Y)_{SS}$ ( $^{\circ}/hr/g^2$ ) is a drift coefficient
$D(X)_{XY^aX^aY}$	gyro drift ( $^{\circ}/hr$ ) about the X axis attributable to the product of accelerations along the X axis and Y axis, where $D(X)_{XY}$ ( $^{\circ}/hr/g^2$ ) is a drift coefficient

$D(Y)_{YX^aY^aX}$	gyro drift ( $^{\circ}/hr$ ) about the Y axis attributable to the product of accelerations along the Y axis and X axis, where $D(Y)_{YX}$ ( $^{\circ}/hr/g^2$ ) is a drift coefficient
$D(X)_{XS^aX^aS}$	gyro drift ( $^{\circ}/hr$ ) about the X axis attributable to the product of accelerations along the X axis and spin axis, where $D(X)_{XS}$ ( $^{\circ}/hr/g^2$ ) is a drift coefficient
$D(Y)_{YS^aY^aS}$	gyro drift ( $^{\circ}/hr$ ) about the Y axis attributable to the product of accelerations along the Y axis and spin axis, where $D(Y)_{YS}$ ( $^{\circ}/hr/g^2$ ) is a drift coefficient
$D(X)_{YS^aY^aS}$	gyro drift ( $^{\circ}/hr$ ) about the X axis attributable to the product of accelerations along the Y axis and spin axis, where $D(X)_{YS}$ ( $^{\circ}/hr/g^2$ ) is a drift coefficient
$D(Y)_{XS^aX^aS}$	gyro drift ( $^{\circ}/hr$ ) about the Y axis attributable to the product of accelerations along the Y axis and spin axis, where $D(Y)_{XS}$ ( $^{\circ}/hr/g^2$ ) is a drift coefficient
$\omega_X$	angular velocity, in inertial space, of the gyro case about the X axis ( $^{\circ}/hr$ )
$\omega_Y$	angular velocity, in inertial space, of the gyro case about the Y axis ( $^{\circ}/hr$ )
hr	sidereal hour
g	local acceleration of gravity, defined positive upward

APPENDIX B

DELTA Curve -  
An Inertial Component Evaluation Concept

Introduction

The technique developed by the author presents a new viewpoint which has proven to be very useful in interpreting inertial sensor test data and in specifying performance. Figure B-1 is a curve for the two-degree-of-freedom Kearfott GYROFLEX Gyro. Once understood, the DELTA Curve provides an excellent tool for gyro performance prediction.

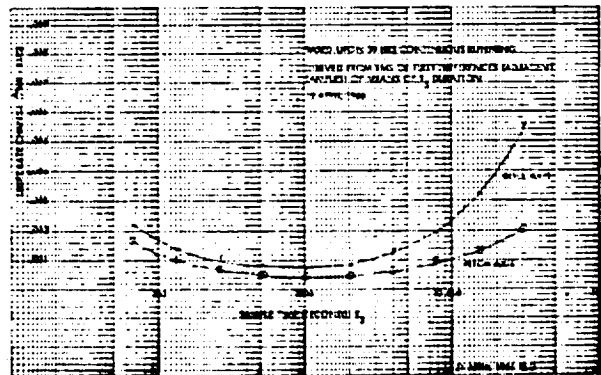


FIGURE B-1. GYROMONITOR EVALUATION--  
DELTA CURVE  
SHORT-TERM PERFORMANCE - GYROFLEX SN 113

The DELTA Curve was created by a need to predict gyro-compassing accuracy when case rotation techniques became known. (B-1) In fact, to construct the curve the data are processed in a technique analogous to the way gyro output data are processed to compute north in the gyrocompass system.

In its broadest sense, the curve is a display of a probable drift rate change of the gyro between mean values of any adjacent samples of gyro output that are of the same duration. The curve shows that the ordinate is a display of the drift rate change and the abscissa represents the sample time. The DELTA Curve is best at displaying the short-term performance of the gyro. For example, in Figure B-1, if the gyro instrumentation output is set to provide samples of 100 second averages, the probable drift rate change between these samples will be .0015°/hr for the pitch axis and .0016°/hr for the roll axis.

The inertial guidance hardware that are most suitable for analysis using this method are those systems which are in some sense self-calibrating. That is, they have a designed-in ability to reject long term or day-to-day bias errors. Hence, methods must be found for predicting system error that describe gyro drift variations during the interval of use instead of how drift changed from the last time the instrument was run (see Figure B-2).

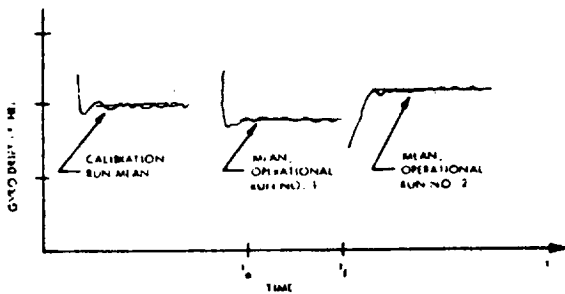


FIGURE B-2. RUN-TO-RUN DRIFT LEVEL CHANGES

### Gyromonitor Inertial Measurement Unit

The gyromonitor inertial platform makes use of a redundant axis of an inertial instrument to calibrate the navigation gyro axes. The monitoring axis is placed parallel to the navigation axis, a discrete sample of both axes outputs is taken and stored. The monitoring axis is then mechanically reversed 180° and a second sample is taken. The data sample pair may then be used to calibrate the navigation axis. The DELTA Curve is a direct measure of gyro stability between adjacent outputs of length  $T_s$ . It has been found that the dead band that appears between samples because of the time required for the 180° reversal does not significantly change the amplitude or shape of the curve. Given the sample time, the system analyst can determine directly the gyro drift contribution; conversely, given a gyro performance requirement, he may determine the required sample time.

### Instrumentation for Data Acquisition

To insure precision and to eliminate human error, a digital output instrumentation loop is recommended. An excellent set-up which is receiving continually greater acceptance is shown in Figure B-3.

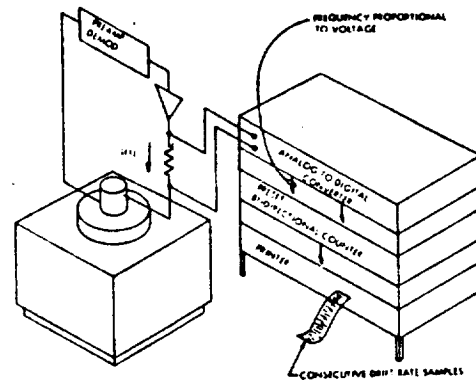


FIGURE B-3. INSTRUMENTATION

The inertial instrument is operated in a capture mode. For the gyro illustrated, current in the "torque-to-balance" loop is proportional to the total rate output  $\omega_T$  of the gyro, i.e.,

$$\omega_T = K_T i(t) = \dot{\theta} + R + \dots$$

where,

$K_T$  = gyro torquer scale factor (°/hr/ma)

$i$  = capture current (ma)

$\dot{\theta}$  = inertial rate sensed by the gyro (dependent upon gyro orientation with respect to earth rate vector)

$R$  = drift coefficient for the gyro (°/hr). Multiple drift terms may be present dependent upon the orientation of the gyro and the complexity of the assumed error model.

The A/D converter detects voltage across a fixed resistor. Proper scaling permits direct printout of rate in degrees-per-hour to obtain the average value of  $\omega_T$  for the selected sample time  $T_s$ .

When we difference consecutive samples, the kinematic rate coupling term  $\dot{\theta}$  is implicitly cancelled and the residual is representative of drift coefficient variation over the interval of the sample pair; for example,

$$\omega_{T_1} - \omega_{T_2} = R_1 - R_2$$

Similarly, the outputs of pulse restrained (captured) instruments may be recorded to accomplish the same purpose. Typically, 5000 or more test data points form the basis for a performance curve which boosts confidence in the statistical significance. Referring back to Figure B-1, we also observe that the optimum smoothing time for this gyro is approximately 1000 seconds wherein the drift rate changes reach the exceptionally low value of .0004°/hr. For sample times longer than 1000 seconds we can see that performance is beginning to degrade as indicated by the positive slope of the curves. This may be justified by the theory of the increasing dominance of instabilities of the gyro and the instrumentation in terms of voltage variations, temperature variations, base motion and other predictable disturbances.

### Construction of the Curve

What we are interested in is the RMS (Root-Mean-Square) value of first differences of constant-interval means ( $\omega_N$ ) of  $T_s$  duration. Sample time  $T_s$  is extended from the shortest sample of interest to the longest sample time that will provide enough first differences to be of statistical significance. This sounds involved so let us take it a step at a time.

First of all, the instrumentation may be adjusted to take the data directly as consecutive average values of drift with the sample time set at the shortest time of interest indicated as  $T_{s1}$ . This technique is graphically sketched in Figure B-4.

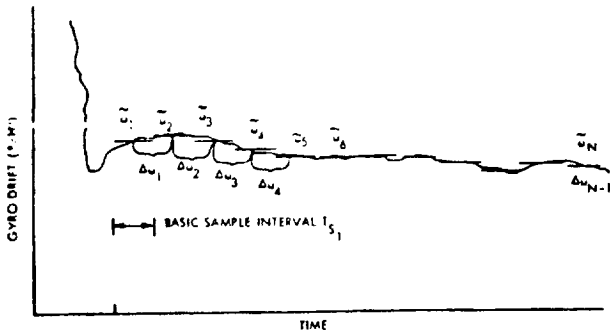


FIGURE B-4. DRIFT RUN PLOT

First differences are simply the differences in the drift value of all adjacent samples, i.e.,

$$\Delta\omega_1 = \omega_1 - \omega_2$$

$$\Delta\omega_2 = \omega_2 - \omega_3$$

or

$$\Delta\omega_N(T_{s1}) = \omega_N - \omega_{N+1}$$

where,

$\tilde{\omega}_N$  = the average value of drift rate, in this case for sample time  $T_{s1}$

The RMS value of all the first differences of drift rate for the sample time  $T_{s1}$  is then calculated in the standard method.

$$\Delta\omega_{rms}(T_{s1}) = \frac{\Delta\omega_1^2 + \Delta\omega_2^2 + \Delta\omega_3^2 + \dots + \Delta\omega_{N-1}^2}{N-1}^{\frac{1}{2}}$$

This is simply the square root of the sum of the squares of individual drift rate differences divided by the number of differences. We now have the first data point for the DELTA Curve. It is plotted at the point labeled  $T_{s1}$  in Fig. B-5.

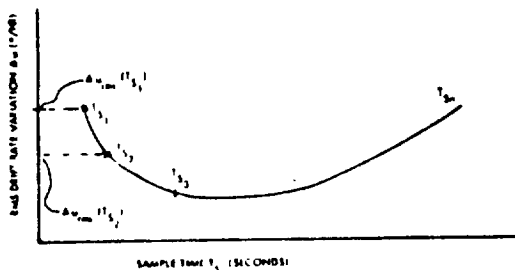


FIGURE B-5. PLOTTING THE FIRST DIFFERENCE CURVE 9

We have gained our first indication of short term gyro performance. Assuming the system is operating by averaging the gyro output for time  $T_{s1}$  (for most of our long gyro runs we set  $T_{s1} = 60$  seconds), the expected change between any consecutive outputs is of the magnitude  $\Delta\omega_{rms}(T_{s1})$  with a probability of about 68% (based upon equating RMS to one sigma).

The next curve point ( $T_{s2}$ ) is obtained using the same basic data that makes up the original drift run. For convenience we double the original sample time to get  $T_{s2}$ . Using the original average drift values, average values for  $T_{s2}$  are calculated; a plot illustrating this is shown in Figure B-6.

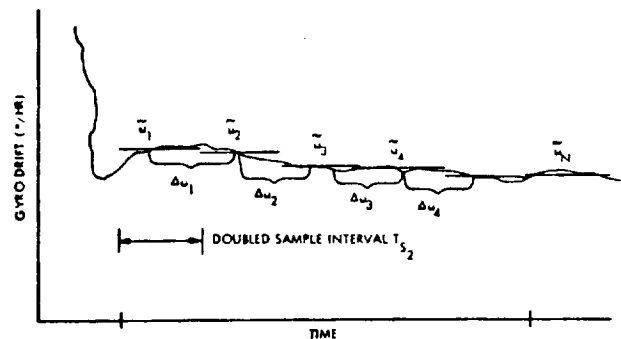


FIGURE B-6. DRIFT RUN - DOUBLED SAMPLE INTERVAL

$$\tilde{\omega}_1(T_{s2}) = \frac{\tilde{\omega}_1(T_{s1}) + \tilde{\omega}_2(T_{s1})}{2}$$

$$\tilde{\omega}_2(T_{s2}) = \frac{\tilde{\omega}_3(T_{s1}) + \tilde{\omega}_4(T_{s1})}{2}$$

$$\tilde{\omega}_N(T_{s2}) = \frac{\tilde{\omega}_N(T_{s1}) + \tilde{\omega}_{N+1}(T_{s1})}{2}$$

Again, first differences are taken and the RMS value for sample time  $T_{s2}$  is calculated forming the second point on the curve.

This process is repeated until the individual samples are so long compared to the total run duration that we have fewer than 5 or so first differences. Thus, for a maximum sample time of one hour, a run of six hours is required for 5 first differences. Of course, the more samples the better the statistical significance of the right side of the curve. Obviously, the number of computations and iterations required suggests a simple computer program for data reduction. It is suggested that all first differences for  $T_{s1}$  be printed on the output listing to permit screening of the data for anomalous data points.

### Transient vs. Steady State Analysis

An interesting method of studying systematic drift effects is possible with the curve. Initially, a DELTA Curve is constructed based upon data taken with the gyro behaving normally in steady state. The systematic drift (such as a ramp

rate function present during warm-up) is then superimposed analytically to construct a composite curve. A parametric composite DELTA Curve can then be used to study acceptable levels for the system.

For example, for a ramp (change in drift rate  $\rho$ /hr/hr), the equation for RMS becomes:

$$\Delta \omega_{rms} = \left[ \frac{\sum_0^{N-1} \Delta \omega_N^2}{N} + \frac{S \Delta T (\sum_0^{N-1} \Delta \omega_N)}{N} + (S \Delta T)^2 \right]^{\frac{1}{2}}$$

New terminology in this equation are:

$S$  = ramp ( $\rho$ /hr/hr)

$\Delta T$  = interval of separation of midpoints of adjacent samples

The middle term can be neglected if the gyro does not have the characteristic of "jogging" and the number of first differences  $N$  is large. Jogging is a step change in drift due to gyro motor disturbances. The equation then simplifies to:

$$\Delta \omega_{rms} = \left[ \frac{\sum_0^{N-1} \Delta \omega_N^2}{N} + (S \Delta T)^2 \right]^{\frac{1}{2}}$$

This equation simply represents the RSS (Root-Sum-Square) of the ramp contribution with DELTA Curve contribution of drift rate. However, this calculation must be made for each point on the curve since  $\Delta T$  changes with sample time. Figure B-7 shows the impact of an  $.03^\circ$ /hr/hr ramp upon a navigation gyro. It is worthy of note that better than  $0.005^\circ$ /hr performance is still present with samples up to 550 seconds duration.

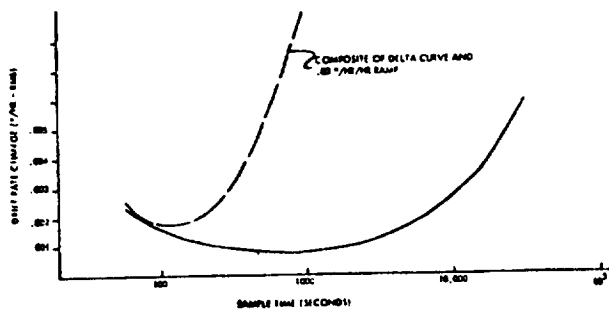


FIGURE 7. NAVIGATION GYRO  
IN PRESENCE OF A RAMP DRIFT

References

- (B-1) Gates, R. L., "Theory of Operation of a Self-Calibrating Gyrocompass", MS Thesis, UCLA, 1963

APPENDIX C

GYRO S/N 606 LONG TERM STABILITY EVALUATION







# MEMORANDUM

TO: SDG Design File  
FROM: T.M. Wirt  
SUBJECT: Gyro S/N 606 Shows A Long Term Trend Of  
.01°/Hour/Year Over A Three Year Period  
REFERENCE:

NO: TMW-2822  
DATE: 13 November 1975

Gyro serial number 606 and its support electronics have been returned after 35 months of extensive testing at NASA's Marshall Space Flight Center and MIT's Draper Labs.

A 30 day repeatability test was started on this unit beginning 28 Oct 75 in the TSC Inertial Labs with a data point (four point-spin axis vertical) to be taken every day. This unit was evaluated in a similar manner in Dec '72 prior to shipping. Comparing the present thirty (30) day test results with those obtained in Dec '72. The following table lists these two test results.

two test results.

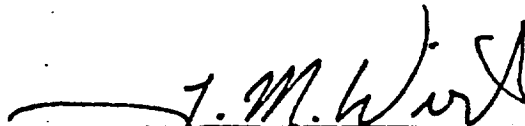
Parameter	Dec '72 Tests	Nov. '75 Tests
Mean value of X-Axis Bias (°/Hr)	-.0057	-.0551
Stand deviation of X-Axis Bias (°/Hr)	.00185	.00167
Mean value of Y-Axis Bias (°/Hr)	.0254	.0403
Stand deviation of Y-Axis Bias (°/Hr)	.00146	.00217
Number of data points	12	30
Test duration (days)	5	34

If the change in bias over that 35 months period is assumed to be a long term trend then the x-axis trend is .0165°/Hr/Year and .0050°/Hr/Year for the Y axis with an average value of .01°/Hr/Year.



It is worthwhile noting that the gyro support electronics contains scaling resistors and buffer amplifiers between scaling resistors and the torquer axes outputs. Thus this bias change includes any offset voltage changes in these buffer amplifiers.

The following pages contain a copy of the Dec '72 test report and a copy of the nov '75 test data to date.

  
T. Wirt

ORIGINAL PAGE IS  
OF POOR QUALITY

STRAPDOWN GYRO PERFORMANCE  
SUMMARY

Part Name: Strapdown Gyro  
Part Number: 8005303-5  
Serial Number: 601  
Date(s) of Test: 12/8/72 . 12/13/72  
Test Console No: B104986

Test Equipment Used:

- 1) Loop closure electronics and test fixture designed by Teledyne and supplied with gyro for test purposes.
- 2) Teledyne Rate Fixture 8008693.
- 3) Electronic counters (2) - Hewlett Packard Model 5325B.
- 4) V-F converters (2) - Hewlett Packard Model 2212A.
- 5) Digital printer - Newport Model 800.
- 6) DC Nullmeters (2) - Hewlett Packard Model 413-AR.
- 7) Chart Recorder - Texas Instruments "Recti/Riter".
- 8) DC Voltage Standard (2) - Analogic Model AN-3100.
- 9) Oven, Delta Design MK2300

CONTRACT NO. NAS8-27452

PERFORMANCE SUMMARY FOR STRAPDOWN GYRO S/N 606

Parameter	Units	Specification	Performance	
			X Axis	Y Axis
1) Random drift (2 hrs)	°/hr (1σ)	.02	.0025	.0029
2) Turn on to turn on repeatability	°/hr (1σ)	.02	.0018	.0015
3) Change of fixed bias over +31°F to +81°F	°/hr(max)	.3	.026	.235
4) Torquer scale factor error over the input range ± 35°/sec	PPM (max)	1000	64	148
5) Maximum input rate (gyro caged)	°/sec	100	100	100
6) Torquer scale factor (minimum value)	°/hr/ma	70	195	195

Test by Paul M. Green Date 12/13/72  
 Q.A. Inspection [Signature] Date 12/13/72

ENTER 1 IF YOU WISH TO USE N-1; ENTER 0 IF YOU WISH TO USE N  
0  
ENTER READINGS AND FREQ. IN DATA STATEMENT FORM (100-200)  
I.E.) 100 DATA 3.5,6,3,2 WHERE 3.5 AND 3 ARE READINGS  
AND WHERE 6 AND 2 ARE FREQ.'S  
WHEN DATA IS ENTERED; TYPE GO TO 90

> 100 DATA 0,2,-.5,1,.7,2,1,1,-1,1,-1.5,1,1.5,6  
> GO TO 90  
ENTER SCALE FACTOR FOR DATA POINTS  
7 .00323  
TOTAL DATA POINTS= 24  
ONE SIGMA VALUE= 2.5427347E-03

ORIGINAL PAGE IS  
OF POOR QUALITY

X AXIS  $\sigma = .00254$

DO YOU WISH TO TRY NEW VALUES? (Y OR N)

DELETE STATEMENTS 100-200  
WHEN DATA IS ENTERED; TYPE GO TO 90

> 100 DATA 0,3,.5,1,-2,4,-2.3,2,-2.2,1,-2.5,13  
> GO TO 90  
ENTER SCALE FACTOR FOR DATA POINTS  
.00302  
TOTAL DATA POINTS= 24  
ONE SIGMA VALUE= 2.869E-03

Y AXIS  $\sigma = .00287$

DO YOU WISH TO TRY NEW VALUES? (Y OR N)

LONG TERM DRIFT

SN 606  
12-12-72



ORIGINAL PAGE IS  
OF POOR QUALITY

TURN-ON TO TURN-ON REPEATABILITY

SN 606  
12-12-72

PROGRAM COMPUTES ONE SIGMA VALUE FOR ANY NUMBER OF INPUTS

ENTER 1 IF YOU WISH TO USE N-1; ENTER 0 IF YOU WISH TO USE N

? 0

ENTER READINGS AND FREQ. IN DATA STATEMENT FORM (100-200)

I.E.; 100 DATA 3.5,6,3,2 WHERE 3.5 AND 3 ARE READINGS

AND WHERE 6 AND 2 ARE FREQ.'S

WHEN DATA IS ENTERED; TYPE GO TO 90

>100 DATA 0,3,-.2,1,.4,2,.7,1,1,1,.5,1,1.5,3

>GO TO 90

ENTER SCALE FACTOR FOR DATA POINTS

? .00306

TOTAL DATA POINTS= 12

ONE SIGMA VALUE= 1.8548511E-03

$X = 1\sigma = .00185$

DO YOU WISH TO TRY NEW VALUES? (Y OR N)

? Y

DELETE STATEMENTS 100-200

WHEN DATA IS ENTERED; TYPE GO TO 90

>100 DATA 0,4,.3,1,-.3,1,.5,1,.7,1,1,4

>GO TO 90

ENTER SCALE FACTOR FOR DATA POINTS

? .00309

TOTAL DATA POINTS= 12

ONE SIGMA VALUE= 1.45664E-03

$Y = 1\sigma = .00146$

DO YOU WISH TO TRY NEW VALUES? (Y OR N)

?

TURN ON TO TURN ON REFLECTABILITY

GYRO CASE TEMPERATURE = 81.5 °F

GYRO SIN COS 12-12-72

X-AXIS  
AIRS (G/HR)  
+0.1  
0  
-0.1

10<sup>-5</sup> = 0.00185

ORIGINAL PAGE IS  
OF POOR QUALITY

Y-AXIS  
G/RS (G/HR)  
+0.1  
0  
-0.1

10<sup>-5</sup> = 0.00146

12-12-72  
JAS



ORIGINAL PAGE IS  
OF POOR QUALITY

FOR THE YEAR 1961  
AND 1962  
AND 1963  
AND 1964

12.8.72



A

FOR THE YEAR 1961 AND 1962 AND 1963 AND 1964

1961-1962  
1963-1964

1965-1966

1967-1968  
1969-1970

1971-1972

1973-1974  
1975-1976  
1977-1978

1979-1980

1981

1982

1983

1984-1985  
1986-1987

ORIGINAL PAGE IS  
OF POOR QUALITY

FOUR POINT SPIN AXIS VERTICAL TEST

DATE 12.8.72 OPERATOR LDK GYRO NO. 606

TEMPERATURE	PRESSURE	GAS	TRIM CAPACITORS
81.5 °F	200 mm Hg	H <sub>2</sub>	X Y
DIS FREQUENCY	P.O. EXCITATION	COVER	P.O. OFFSETS
		SEALED	ΔX <.5 SEC ΔY <.5 SEC
SPIN FREQUENCY	MOTOR	TORQUER	P.O. POT SETTINGS
900.00	30 VOLTS WATTS	C	P <sub>X</sub> 505.1 P <sub>Y</sub> 507.1

POSITION	TABLE READING	POSITION DESCRIPTION	X <sub>n</sub> (MA)	Y <sub>n</sub> (MA)
1	0° 15'	X <sub>T</sub> NORTH, Y <sub>T</sub> EAST	-0.00009	+0.06198
2	270° 15'	X <sub>T</sub> EAST, Y <sub>T</sub> SOUTH	+0.06235	+0.00003
3	180° 15'	X <sub>T</sub> SOUTH, Y <sub>T</sub> WEST	+0.00004	-0.061715
4	90° 15'	X <sub>T</sub> WEST, Y <sub>T</sub> NORTH	-0.06245	+0.00023
1	0° 15'	X <sub>T</sub> NORTH, Y <sub>T</sub> EAST	-0.00010	+0.06198

COMMENTS: Para. 6.0 & 6.1 OF ATP

F79381-2

LDK

INPUT RATE ABOUT Y

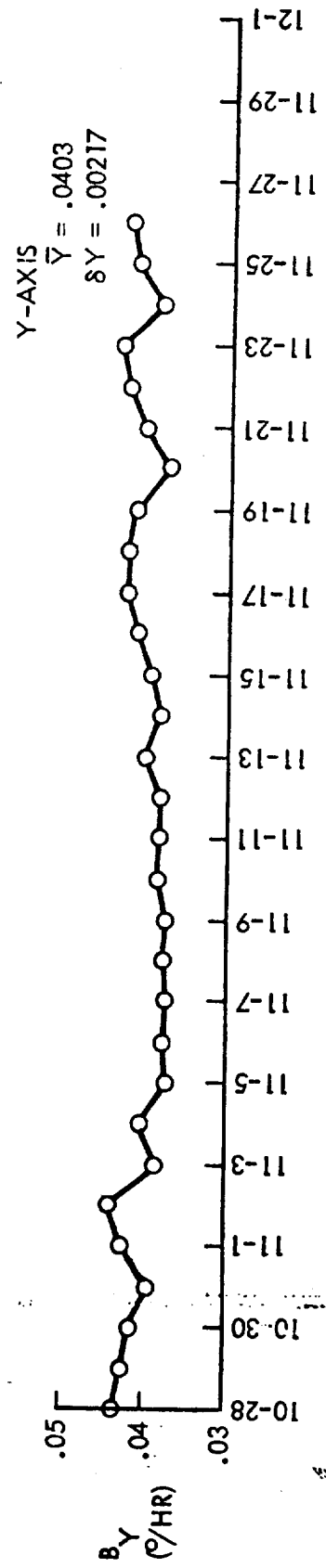
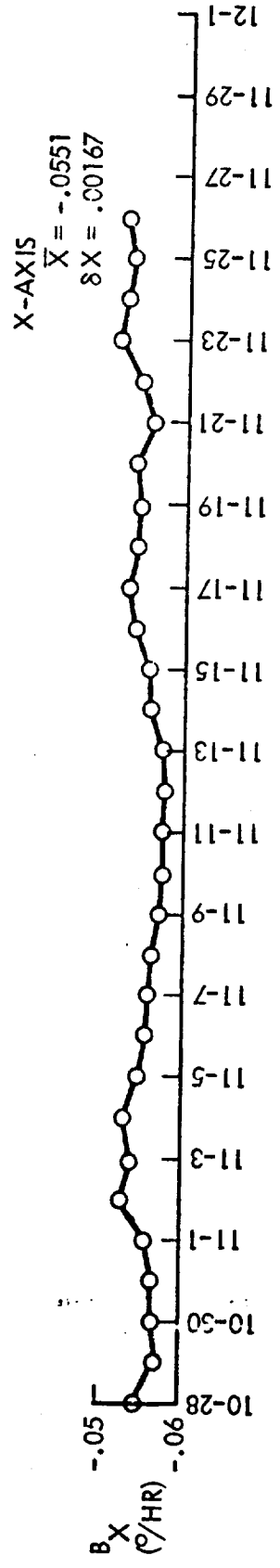
Y AXIS

AXIS

INPUT RATE (°/sec)	COUNTS /REV.	AVERAGE COUNTS/REV.	TIME/REV. (sec.)	AVERAGE TIME/REV. (sec)	DRIVING VOLTS TO TABLE	SCALE FACTOR (°/sec/VOLT)	FIXTURE (°F)
36.625 624	+	1720160		9.829184	1	21	
36.612 789	-	1720836		9.83263	1	20.725	257
36.1170	+	1708278		170.36345	1	21.120	197
36.1131	-	-1702530		170.34217	1		
21.1221	+	-1704499		17.04378	1	21.120	15
21.1222	-	-1704533		17.04369	1		
12.2414	+	1701502		8.52245	1	21.120	43
12.2404	-	-1704648		8.52265	1		

30 DAY BIAS REPEATABILITY  
S/N 606

DATA REDUCED FROM 4-POINT  
SPIN AXIS VERTICAL TEST



T101522